Geological Magazine

www.cambridge.org/geo

Revisiting the phosphorite deposit of Fontanarejo (central Spain): new window into the early Cambrian evolution of sponges and the microbial origin of phosphorites

Joachim Reitner[1,2], Cui Luo[3], Pablo Suarez-Gonzalez[4] and Jan-Peter Duda[2,5]

[1]Department of Geobiology, Centre of Geosciences of the University of Göttingen Goldschmidtstraße 3, Göttingen, Germany; [2]Academy of Science and Humanities, Theater Str. 7, 37077 Göttingen, Germany; [3]State Key Laboratory of Palaeobiology and Stratigraphy, Nanjing Institute of Geology and Palaeontology and Center for Excellence in Life and Paleoenvironment, Chinese Academy of Sciences, 39 East Beijing Road, Nanjing 210008, China; [4]Departamento de Geodinámica, Estratigrafía y Paleontología, Universidad Complutense de Madrid, C/José Antonio Novais 12, 28040 Madrid, Spain and [5]Sedimentology & Organic Geochemistry Group, Department of Geosciences, Eberhard-Karls-University Tübingen, Schnarrenbergstraße 94-96, 72076 Tübingen, Germany

Original Article

Cite this article: Reitner J, Luo C, Suarez-Gonzalez P, and Duda J-P (2022) Revisiting the phosphorite deposit of Fontanarejo (central Spain): new window into the early Cambrian evolution of sponges and the microbial origin of phosphorites. *Geological Magazine* **159**: 1220–1239. https://doi.org/10.1017/S001675682100087X

Received: 3 December 2020
Revised: 24 July 2021
Accepted: 28 July 2021
First published online: 29 September 2021

Keywords:
Lower Cambrian; Porifera; Hexactinellida; Demospongiae; microbialites

Author for correspondence:
Joachim Reitner,
Email: jreitne@gwdg.de

Abstract

Fossils within early Cambrian phosphorites worldwide are often well preserved due to early diagenetic permineralization. Here, we examine the fossil record contained within phosphorites of the Lower Cambrian Pusa Formation (late Fortunian to Cambrian Stage 2) in Fontanarejo, central Spain. The sedimentology and age of these phosphorites have been controversial and are here reviewed and discussed, providing also an updated geological map. The Pusa Formation is composed of fine clastic sediments that are partly turbiditic, with channels of quartz-rich conglomerates and abundant phosphorites in the upper part of the succession. The microfacies and mineralogy of these channel deposits are studied here for the first time in detail, showing that they are mainly composed of subspherical apatite clasts, with minor mudstone intraclasts, quartzite and mica grains. Numerous sponge spicules, as well as entirely preserved hexactinellid sponges and demosponges, were collected within these phosphorites and likely represent stem groups. In addition to sponges, other fossils, such as small shelly fossils (SSF) of the mollusc *Anabarella* sp., were found. The phosphorites exhibit multiple evidence of intense microbial activity, including diverse fabrics (phosphatic oncoidal-like microbialites, thrombolites, stromatolites and cements) and abundant fossils of filamentous microbes that strongly resemble extant sulphur-oxidizing bacteria. Our findings strongly suggest that microbial processes mediated the rapid formation of most of the Fontanarejo apatite, probably accounting for the exceptional preservation of fragile fossils such as sponge skeletons. The apparent presence of taxonomically diverse hexactinellid and demosponge communities at the lowermost Cambrian further corroborates a Precambrian origin of the phylum Porifera.

1. Introduction

The poor early fossil record makes investigations of sponge evolution difficult. Ediacaran sponge-like fossils are questionable (e.g. Gehling & Rigby, 1996; Brasier *et al.* 1997; Li *et al.* 1998; Reitner & Wörheide, 2002; Maloof *et al.* 2010; Antcliffe *et al.* 2014), and the earliest appearance of sponge spicules has been dated to *c.* 535 Ma (Guo *et al.* 2008; Chang *et al.* 2017). Problematically, however, disarticulated spicules are of little taxonomic value. To date, articulated, well-preserved sponge fossils in Burgess-Shale-type preservation and deep-water black shales have only been reported after the beginning of Cambrian Age 3 (e.g. Steiner *et al.* 1993; Luo *et al.* 2020). Furthermore, Luo & Reitner (2019) described three-dimensionally preserved sponge skeletal frames from the basal Niutitang Formation (Stage 2) near Sancha in China that have illuminated the nature of stem-group hexactinellids.

Here, new occurrences of sponge fossils of no later than the Cambrian Age 2 are described from phosphorite deposits near the village of Fontanarejo in central Spain (Fig. 1). The Fontanarejo phosphorites belong to the Pusa Formation and were targets of mining exploration led by the Geological Survey of Spain (IGME). Perconig *et al.* (1983, 1986) provided the first summary of the formation's stratigraphy, sedimentology and fossil content (particularly sponge spicules) in Fontanarejo. While these early studies considered the Fontanarejo phosphorites to be of Ediacaran age, Jensen *et al.* (2010) suggested a Lower Cambrian age (Fortunian) for the Pusa Formation. Reitner *et al.* (2012) and Reitner & Luo (2019) provided the first overview of the different sponge types contained within the Fontanarejo deposits, highlighting their stratigraphic value. The aim of this paper is to describe the different types of sponge remains found in the Fontanarejo phosphorites in greater detail and to discuss them in a taxonomic frame

CAMBRIDGE UNIVERSITY PRESS

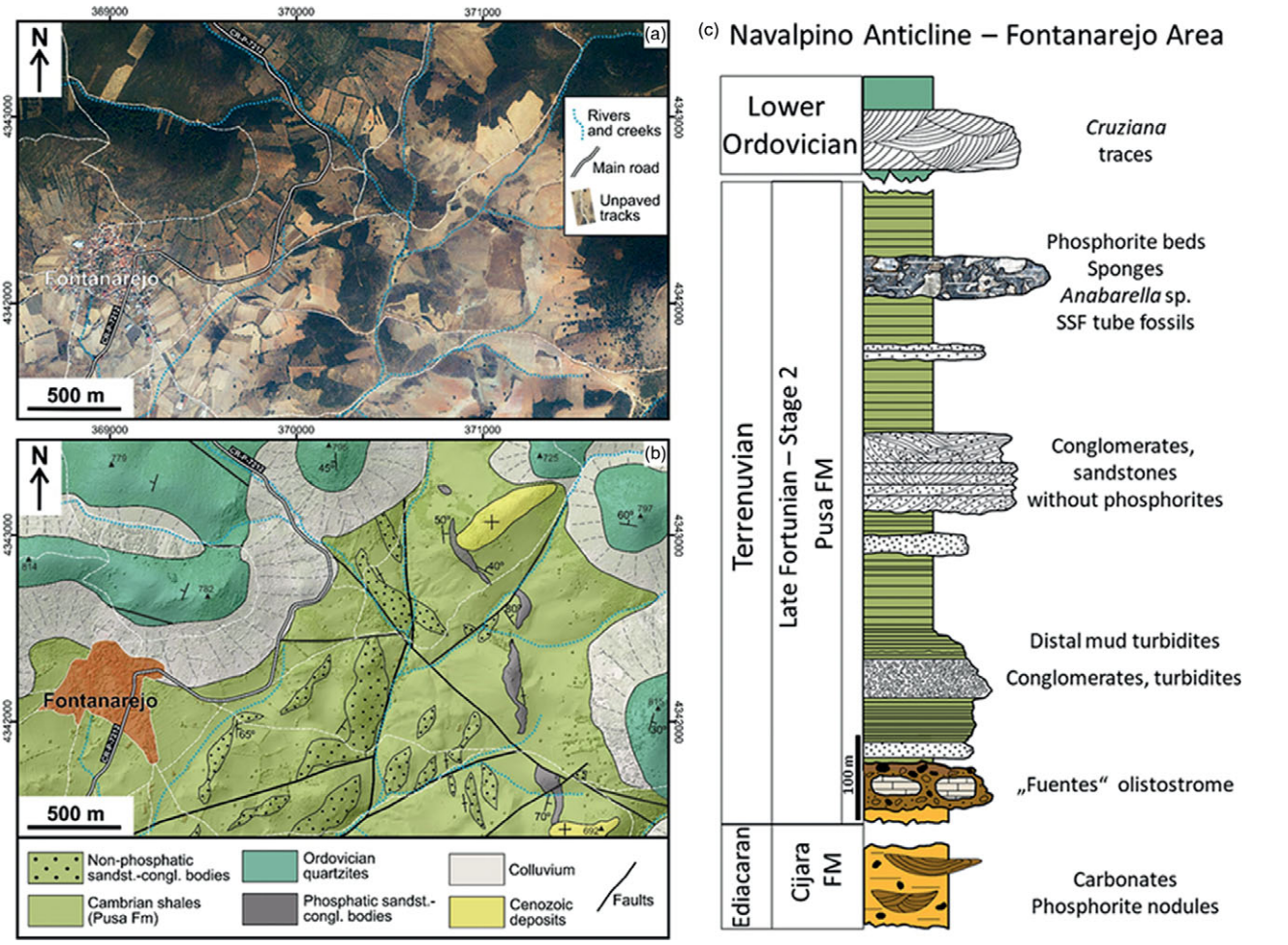

Fig. 1. (a) Latest available orthophotograph (2019) of the Fontanarejo area (obtained from the Spanish Geographical Survey, IGN) showing the current outcrop conditions, dominated by vegetation and agricultural lands. (b) Geological map of the Fontanarejo area, same extension as in (a), at the western end of the Navalpino Anticline. Map is drawn over a lidar digital elevation model (obtained from the Spanish Geographical Survey, IGN) and based on our own fieldwork and on the previous geological maps of the area. (c) Reconstructed stratigraphic section of the Fontanarejo area, based on Perconig *et al.* (1986), Picart Boira (1988) and our own fieldwork. The Ediacaran Cijara Formation and the so-called 'Fuentes' olistostromes (base of the Pusa Formation), which roughly represent the Precambrian–Cambrian boundary, are not exposed in this area. Data used in this reconstruction are from Álvaro *et al.* (2016) and Jensen *et al.* (2010). This section shows the stratigraphic base, which is exposed in the Valdelacasa Anticline west of Fontanarejo.

advocated by the authors. In addition to sponges, other fossils recovered from the phosphorites, including small shelly fossils (SSF) and microbial fossils, were studied. A further goal of the paper is to examine the microbial impact on early diagenetic apatite formation that facilitated the exceptional preservation of fossils.

Assuming that animal life had a long evolutionary history before the Cambrian, palaeontologists have been tracing the earliest fossil evidence of sponges for many decades. Putative Precambrian spicule-like structures have been reported from analyses of thin-sections (e.g. Brasier *et al.* 1997; Li *et al.* 1998; Reitner & Wörheide, 2002) and macroscopic Ediacaran fossils (e.g. Gehling & Rigby, 1996; Serezhnikova & Ivantsov, 2007; Clites *et al.* 2012). Furthermore, enigmatic structures observed in various Neoproterozoic successions were interpreted to be poriferan (e.g. Maloof *et al.* 2010; Brain *et al.* 2012; Wallace *et al.* 2014). These microscopic and macroscopic structures have mostly been discounted by later studies (e.g. Antcliffe *et al.* 2014; Muscente *et al.* 2015; Cunningham *et al.* 2016; Luo *et al.* 2017). The most plausible alternative evidence for Precambrian sponges, i.e. molecular fossils (e.g. Love *et al.* 2009; Zumberge *et al.* 2018) and exceptionally preserved fossils from the Weng'an Biota (Yin *et al.* 2015), is also still under debate (e.g. Antcliffe *et al.* 2014; Botting & Muir, 2018).

Several reasons may plausibly explain the poor fossil record of early sponges. For instance, the earliest sponges may have been too small or too labile to be fossilized, or they were morphologically very different from their Phanerozoic descendants.

Regardless of this question, the earliest indisputable sponge fossils are disarticulated spicules recognized from the Fortunian (538.8–529.0 Ma; Peng *et al.* 2020). These fossil spicules include pentactins and hexactins macerated from the *Protoherzina* biozone of the Yangjiaping Formation of Hunan, China (Ding & Qian, 1988), and stauractins and pentactins from the same biozone of the Soltanieh Formation in North Iran (Antcliffe *et al.* 2014). The spicules from Iran occur right above the Basal Cambrian Carbon Isotope Excursion (BACE). Probably even earlier occurrences of spicules were reported from the Yanjiahe Formation of Yangtze Gorges which were correlated to around the nadir of the BACE, although the referred geochemical profiles were not

https://doi.org/10.1017/S001675682100087X Published online by Cambridge University Press

directly obtained from the fossil-bearing outcrop (Chang *et al.* 2017, 2019).

Taxonomically more informative sponge fossils (i.e. those preserved with articulated skeletal frames) are mostly known from fossil Lagerstätten that slightly predate the Cambrian Age 3. Famous examples include black shales of the Niutitang and Hetang Formations in South China (Steiner *et al.* 1993; Xiao *et al.* 2005), the Chengjiang Biota (e.g. Chen *et al.* 1989, 1990; Rigby & Hou, 1995), the Sirius Passet Biota (Botting & Peel, 2016) and the Burgess Shale fossil Lagerstätte (e.g. Rigby, 1986; Rigby & Collins, 2004). The recently described three-dimensionally preserved hexactinellid sponge fossils and diverse disarticulated spicules from cherty phosphorites at the basal Niutitang Formation of Hunan, China, are probably older than 521 Ma, thus providing a valuable window for studying sponge palaeobiodiversity, palaeoecology and evolution preceding the Cambrian Epoch 2 (Luo & Reitner, 2019).

The Fontanarejo Lagerstätte is of similar age to – or perhaps slightly older than – the Niutitang phosphorites as indicated by recent discoveries of *Anabarella* and an improved sedimentological correlation (Álvaro *et al.* 2019; Álvaro & Lorenzo, 2021; this study). It therefore provides unique and valuable insights into early metazoan diversity, particularly allowing for the reconstruction of the major sponge branches.

Sponges are famous for their morphological plasticity and richness of homoplastic characters. The fact that even these characters were only partly preserved in fossils increases the difficulty of establishing a natural classification for distinct taxa, which is one of the major objectives of palaeontological research. Generally, the classification used here follows the traditional concept of the *Systema Porifera: A Guide to the Classification of Sponges* (Hooper & Van Soest, 2002). Recent phylogenomic studies have partly challenged the sponge taxonomy advocated in this book (e.g. Morrow & Cárdenas, 2015; Erpenbeck *et al.* 2020). Nevertheless, it is still the best reference work for palaeontologists because it is based on a balanced consideration of both morphological and molecular features. For this reason, we integrate findings from the most recent phylogenetic models (e.g. Erpenbeck & Wörheide 2007; Dohrmann *et al.* 2008; Wörheide *et al.* 2012; Redmond *et al.* 2013) into the taxonomic frame of Hooper & van Soest (2002).

A different phylogenetic framework for sponges has recently been proposed by Botting & Muir (2018). This concept, however, is not adopted here since the underlying data require re-examination and some key phylogenetic interpretations need further discussion. For example, the authors stated that a tetraradial symmetry was ancestral to all sponges but secondarily lost. This is neither supported by phylogenetic analyses of living sponges, nor by sufficient palaeontological evidence except for a superficial similarity between the Burgess Shale fossil *Takakkawia* and the ctenophore *Thaumactena ensis* from the Chengjiang Biota. In fact, some phylogenetically distant modern sponge taxa show tetraradial symmetry, such as the hexactinellid *Composocalyx* (Tabachnick & Menshenina 2002) and the carnivorous demosponges *Chondrocladia lyra* (Lee *et al.* 2012). The latter even exhibits other symmetrical patterns within the single species, including bilateral, triradial and pentaradial forms, and, this seems to be of ecological rather than phylogenetic significance (e.g. Tabachnick, 1991). Indeed, these symmetrical patterns are absent in closely related lineages of the symmetric taxa (Morrow & Cárdenas, 2015; Dohrmann *et al.* 2017). From a palaeontological point of view, there is obviously no robust evidence to support the claim that Cambrian tetraradial sponges evolved earlier than other fossil taxa. A detailed account of the controversy surrounding this new phylogenetic frame is beyond the scope of this paper and will be discussed in future publications.

2. Material and methods

Over the last two decades, we conducted several field campaigns to the phosphorite deposits in the Fontanarejo area, with the aim of mapping the outcrop and collecting samples. In the field, we collected data for preparing a new geological map of the area, using previous maps as a starting point (Perconig *et al.* 1983, 1986; Monteserín López *et al.* 1989; López Díaz, 1995) (Fig. 1). The background geographic information used was the latest available topographic maps, and lidar digital elevation models, obtained from the Spanish Geographical Survey (IGN) in 2019. The geographic data were processed and managed using QGIS software, and the geological map was drawn using CorelDraw.

Additional photos of the outcrop geology and deposits are provided in Supplementary Figures S1 and S2 (in the Supplementary Material available online at https://doi.org/10.1017/S001675682100087X).

We collected more than 200 rock samples in the field. From these, we prepared 120 large thin-sections (10 × 5 cm, 5 × 5 cm, and 15 × 10 cm). The thin-sections are archived in the museum collection of the Faculty of Geoscience and Geography at the University of Göttingen, Germany (inventory number GZG.INV.808).

Thin-section analyses were conducted using a Zeiss SteREO Discovery.V12 stereo microscope and a Zeiss AxioImager Z1 microscope. Both microscopes were connected to a Zeiss AxioCam MRc camera. A fluorescence microscope equipped with an ebx 75 isolated power unit was mounted on a Zeiss AxioImager Z1 microscope. The instrument was fitted with a Zeiss A 10 Alexa Fluor 488 filter, with an excitation wavelength of BP 450–490 nm and an emission wavelength of BP 515–565 nm. For cathodoluminescence (CL) microscopy, a Cambridge Instrument Citl CCL 8200 Mk3A cold-cathode system (operating voltage of *c.*15 kV; electric current of *c.* 250–300 μA) linked to a Zeiss Axiolab microscope and AxioCam 703 camera was used. Field emission scanning electron microscopy (Fe-SEM) was performed with a Carl Zeiss LEO 1530 Gemini system. The instrument was coupled to an Oxford Instruments INCA X-act energy-dispersive X-ray spectrometry (EDX) detector, to additionally obtain EDX single spectra and elemental maps.

Elemental distributions in the phosphorite samples were mapped using a Bruker M4 Tornado micro X-ray fluorescence (μ-XRF) instrument equipped with a XFlash 430 Silicon Drift Detector. Analyses were carried out at a spatial resolution of 70 μm. Each pixel covers 30 ms. Measurements were performed at 50 kV and 400 μA at a chamber pressure of 20 mbar. Additionally Raman spectroscopy was used for point measurements and area mapping. Raman spectra were collected using a WITec alpha300 R fibre-coupled ultra-high throughput spectrometer. Before analysis, the system was calibrated using an integrated light source. The experimental set-up included a 405 nm laser (chosen to reduce fluorescence effects), 10 mW laser power, and 50x and 100x long working distance objectives with a numerical aperture of 0.55 and a grating of 1200 g mm^{-1}. This set-up had a spectral resolution of 2.6 cm^{-1}. The spectrometer was centred at 1530 cm^{-1}, covering a spectral range from 122 cm^{-1} to 2759 cm^{-1}. Each spectrum was collected by two accumulations, with an acquisition time of 5 s. Raman spectra were processed with

https://doi.org/10.1017/S001675682100087X Published online by Cambridge University Press

the WITec project software. The background was subtracted using a rounded shape, and band positions were determined by fitting a Lorentz function. Both analytical facilities (μ-XRF and Raman spectroscopy) are located at the Geosciences Center of the University of Göttingen. Detailed μ-XRF and Raman maps are provided in Supplementary Figures S3–S5 (in the Supplementary Material available online at https://doi.org/10.1017/S001675682100087X).

3. Regional geology and stratigraphy

3.a. Regional geological setting

The studied deposits crop out near the village of Fontanarejo (Ciudad Real province, central Spain) (Fig. 1). Geographically, the successions are located at the southern margin of the Toledo Mountains, and geologically they are part of the southeast area of the Central Iberian Zone (CIZ) of the Iberian Variscan Massif. This area of the CIZ consists of large-scale, NW–SE-trending upright folds, topographically highlighted by the relief of the Ordovician quartzites. The folds include wide anticlines containing pre-Ordovician materials and narrower synclines containing Ordovician–Devonian deposits (Díez Balda *et al.* 1990; Vidal *et al.* 1994; Liñán *et al.* 2002; Valladares *et al.* 2002; Martínez Catalán *et al.* 2004; Álvaro *et al.* 2019). The Fontanarejo area represents the northeastern border of the Navalpino Anticline, which accordingly exhibits a core of folded and deformed Neoproterozoic and Cambrian rocks unconformably overlain by Ordovician quartzites (San José, 1984; López Díaz, 1994, 1995; Gutiérrez-Marco *et al.* 2017) (Fig. 1b, c; Supplementary Fig. S1, in the Supplementary Material available online at https://doi.org/10.1017/S001675682100087X). The studied phosphate-rich deposits are part of the Cambrian succession that directly underlies the Ordovician quartzites of the northeastern margin of the Navalpino Anticline (cf. Perconig *et al.* 1983, 1986; Picart Boira, 1988) (Fig. 1b, c; Supplementary Fig. S1. in the Supplementary Material available online at https://doi.org/10.1017/S001675682100087X).

3.b. Stratigraphy

The stratigraphic terminology and age of the pre-Ordovician deposits of the CIZ have been controversial for several decades (see discussions in San José *et al.* 1990; Vidal *et al.* 1994; Rodríguez Alonso *et al.* 2004; Jensen *et al.* 2010; Álvaro *et al.* 2019). Typically, these deposits have been divided into three large lithostratigraphic units, with varying names and boundaries. The Fontanarejo phosphorites belong to the youngest of these groups, termed 'Pusian' (San José *et al.* 1990), 'Valdelacasa Group' (Monteserín López *et al.* 1989) or 'Río Huso Group' (Vidal *et al.* 1994). Within this group, the studied deposits belong to a shale-dominated unit termed the Pusa Formation, whose composition and boundaries have also been studied previously (e.g. San José *et al.* 1990; Vidal *et al.* 1994; Álvaro *et al.* 2019).

From a sedimentological point of view, the Pusa Formation in the study area has six sequences or subunits (San José, 1984; Gabaldón López *et al.* 1989), with the Fontanarejo phosphorites being part of subunit 5. San José (1984) even defined them as a member within the unit ('Fontanarejo Member'). From a cartographic point of view, the Pusa Formation has only two (Monteserín López *et al.* 1989) or three (San José, 1984; López Díaz, 1994; Vidal *et al.* 1994) mappable subunits. The latest stratigraphic review (Álvaro *et al.* 2019) considers three mappable lithostratigraphic members, with the Fontanarejo phosphorites being part of the middle, conglomerate-rich member (Fig. 1c; Supplementary Fig. S1, in the Supplementary Material available online at https://doi.org/10.1017/S001675682100087X). According to this recent stratigraphic framework, the Pusa Formation is as thick as 3500 m. Lithologically, the formation is dominated by shales interbedded with breccia, conglomerates and sandstones, but also locally contains carbonate and phosphorite seams (Álvaro *et al.* 2019).

The precise age of the Pusa Formation remains uncertain, but most interpretations agree that it includes deposits from the latest Neoproterozoic and earliest Cambrian (Brasier *et al.* 1979; Perconig *et al.* 1983, 1986; San José, 1984; Monteserín López *et al.* 1989; Vidal *et al.* 1994; Jensen *et al.* 2010). However, a zircon age of 533 ± 17 Ma from the middle part of its lower member (Talavera *et al.* 2012), and the discovery of *Anabarella* cf. *plana* fossils, have led the Pusa Formation to be assigned exclusively to the Lower Cambrian, mainly to the Terreneuvian. The presence of trilobites, small shelly fossils and archaeocyaths evidences that the stratigraphic position of the upper Pusa Formation corresponds to the Cambrian Series 2 (Álvaro *et al.* 2019).

Notably, we also found *Anabarella*-like fossils within the Fontanarejo phosphorite deposits. This finding aligns with occurrences of *Anabarella* cf. *plana* in stratigraphically equivalent sedimentary rocks from the Alcudia anticline close to Ciudad Real in central Spain (i.e. 'Conglomerados de San Lorenzo', Pusa or Fuentepizarra formations: Pieren & García-Hidalgo, 1999; Vidal *et al.* 1999; Pieren Pidal, 2000; Álvaro *et al.* 2019; Álvaro & Lorenzo, 2021). Given this stratigraphic framework, the phosphorite deposits of Fontanarejo we studied are likely late Fortunian – earliest Age 2 in age. Figure 1c summarizes the main sedimentary structures and the stratigraphy of the Fontanarejo area.

4. Outcrop description and sedimentology

The landscape of the Fontanarejo area is mainly controlled by the weathering susceptibility of shales from the Pusa Formation underlying the main agriculture fields (Fig. S1, in the Supplementary Material available online at https://doi.org/10.1017/S001675682100087X). Interbedded with the shales are more weathering-resistant sandstone–conglomerate beds that form the small hills of the landscape. The phosphorites we studied crop out ~2 km east of the village of Fontanarejo and are embedded in the youngest series of the sandstone–conglomerate beds (Perconig *et al.* 1983, 1986; Picart Boira, 1988) (Fig. 1b, c; Supplementary Figs S1, S2, in the Supplementary Material available online at https://doi.org/10.1017/S001675682100087X). These phosphorite deposits were first identified in the course of extensive field campaigns conducted by IGME during the 1980s. Since then, the Fontanarejo outcrops have been significantly degraded due to agricultural activities (Supplementary Fig. S1). This makes it almost impossible to find *in situ* outcrops larger than a couple of square metres, and those are significantly weathered. A further problem is that different phosphorite beds cannot be directly correlated due to fault displacement.

Given the current poor outcrop conditions, it is difficult to accurately assess the geometry and macroscopic features of the sandstone–conglomerate beds in greater detail. However, they are clearly discontinuous and locally seem to pinch out laterally. Furthermore, they appear to be 100–500 m wide and 20–70 m thick. All these characteristics are consistent with the previous descriptions of the surface and subsurface. Notably, earlier studies have reported that some of the beds display erosional bases and flat

to undulated tops and internally include fining-upward, cross-bedded sediments (Perconig *et al.* 1983, 1986; Picart Boira, 1988; Álvaro *et al.* 2016). We found these features only to be present in sandstone–conglomerate beds that do not contain a significant number of phosphorite pebbles (Supplementary Fig. S2e, in the Supplementary Material available online at https://doi.org/10.1017/S001675682100087X), while they appear to be absent in the youngest, phosphorite-rich beds in the succession (Supplementary Figs S1, S3). Regardless of these differences, however, integrated map and field evidence suggests that the phosphorite-rich and phosphorite-poor bodies are both channel deposits.

Detailed microfacies analyses of the youngest, phosphate-rich sandstone–conglomerate beds revealed that these deposits exhibit a typical rudstone fabric (Supplementary Figs S1d, S3, in the Supplementary Material available online at https://doi.org/10.1017/S001675682100087X). About 90 % of the beds consist of phosphate clasts that are ovoidal to subspherical in shape and display black, grey and brown colours. The remaining 10 % comprise reworked, sub-rounded blocks of Pusa shale, often containing angular grey mudstone intraclasts and quartzite grains with minor mica. Iron oxide crusts surround many phosphate clasts and are likely remnants of former framboidal pyrites. Two types of phosphatic sediments are present: one is more weathered and iron oxide rich, the other is fresher, with black to grey clasts with less iron oxide.

The phosphate clasts consist of apatite and display diverse morphologies. Ovoid-shaped clasts, some millimetres in size ('oncoid-like microbialites'), are abundant and have distinct nuclei. They are often composed of sponge remains, SSF relics and mud clasts. Anatase (TiO_2) is common and often associated with microbial remains, rendering an authigenic origin possible. The oncoid-like microbialites do not show any clear laminated fabric but instead display cloudy colloform, often thrombolitic structures that are enriched in organic matter. Clay minerals form the nucleic area of the oncoid-like microbialites (Supplementary Fig. S3, in the Supplementary Material available online at https://doi.org/10.1017/S001675682100087X).

In addition to the oncoid-like microbialites, mm-sized microcrystalline structureless apatite clasts are also common and often include sponge spicules. The microcrystalline apatite components usually show shrinkage patterns and are brown or dark grey in colour. The spicule-rich apatite, in contrast, has an irregular shape, is generally honey-yellow in colour and is locally enriched in organic matter. Such micro-peloidal textures typically result from the taphonomic mineralization of microbially interspersed sponge tissue (Reitner & Neuweiler, 1995; Reitner & Schumann-Kindel, 1997). For this reason, we interpret these components as permineralized sponge tissue.

Early diagenetic phosphatic cements are quite common. Early fibrous prismatic phosphatic cements surround spicules and other components. This early cementation also locally stabilized and preserved original spicule arrangements, facilitating the interpretation of the sponge fossils. Later diagenetic phosphatic cements exhibit larger crystals, and it seems that phosphate minerals replaced siliceous (spicules) and calcareous materials (cf. Perconig *et al.* 1983, 1986; Picart Boira, 1988; Álvaro *et al.* 2016).

Most studies interpret the Fontanarejo phosphorites (and equivalent deposits in adjacent areas) as allochthonous channel deposits formed in an offshore shelf/platform setting, below wave base level, probably close to the platform margin or to the beginning of the slope (Picart Boira, 1988; Gabaldón López *et al.* 1989; Pieren Pidal, 2000; Álvaro *et al.* 2016). However, Perconig *et al.* (1983, 1986) interpreted the Fontanarejo phosphorites as intertidal and subtidal channel deposits, based on the sorting and rounding of the clasts, the biogenic features recognized in the rocks, and the local presence of mud cracks. Our findings clearly support the first, more traditional interpretation. This conclusion is based on map and field evidence as well as on microfacies characteristics (see above). For instance, we found no sedimentological evidence for subaerial exposure (e.g. mud cracks). Furthermore, the channel infill is polymictic and poorly sorted, suggesting relatively rapid sedimentation after high-energy episodes that remobilized material from shallower areas as well as material from adjacent zones. The interpretation that some of the Pusa shales are distal mud turbidites interbedded with channels and turbiditic sandstone layers (Fig. 1c; Supplementary Fig. S2a, b, d, in the Supplementary Material available online at https://doi.org/10.1017/S001675682100087X) is consistent with findings from other studies on the formation (San José, 1984; Monteserín López *et al.* 1989; López Díaz, 1994; Vidal *et al.* 1994; Rodríguez Alonso *et al.* 2004; Álvaro *et al.* 2016, 2019).

5. Results and discussion: Animal fossils in Fontanarejo phosphorites

5.a. Phylogenetic status of Hexactinellida (Schmidt, 1870)

As outlined in the Introduction and discussed below, it is overwhelmingly difficult to reconstruct the phylogeny of fossil sponges. Therefore, our study is based on the careful examination and morphological classification of fossil sponge remains contained in the investigated materials.

Hexactinellids are a monophyletic group characterized by triaxon spicules. Based on distinct microscleres, two major clades are defined in this class: Hexasterophora and Amphidiscophora (Schulze, 1886). The ancestral hexactinellid spicule was interpreted to be regular hexactin (Reitner & Mehl, 1996; Dohrman *et al.* 2008, 2017). It has long been debated how the palaeontological record can be reconciled with modern molecular phylogenetic data. The skeletal architecture of early Palaeozoic hexactinellids includes two major morphological groups, the Reticulosa Reid, 1958 and the 'Rossellimorpha' (Mehl, 1996), both of which could be paraphyletic or polyphyletic (Mehl-Janussen, 1999; Botting & Muir, 2018).

Most of the Fontanarejo articulated hexactinellid sponges exhibit a lyssacine body plan, i.e. a primarily non-cemented spicular skeleton. These early lyssacine hexactinellids fit best with the morphological group 'Rossellimorpha A' defined by Mehl-Janussen (1999). Some Fontanarejo hexactinellids display a cemented skeleton resembling a type of 'dictyonal' body plan (description see Section 5.b), in which the spicules are cemented by controlled secondary silica cementation. This type of skeleton may have evolved independently and therefore represent a polyphyletic characteristic. Steiner *et al.* (1993) reported the first more typical dictyonal hexactinellid from China (*Sanshadictya microreticulata* Mehl & Reitner 1993), which also has an early Cambrian (Age 3) age. To date, the earliest convincing modern-type dictyonal skeletons are of middle Devonian age (Mehl, 1996).

5.b. Fontanarejo hexactinellid spicule record

Most of the observed hexactinellid spicules are adaptions of simple hexactins (Fig. 2). The average size of the spicules is *c.* 500 µm. Many of these show a residual axial canal that originally contained a protein-rich organic fibre but now is often filled with iron oxide, likely resulting from the diagenetic alteration of primary

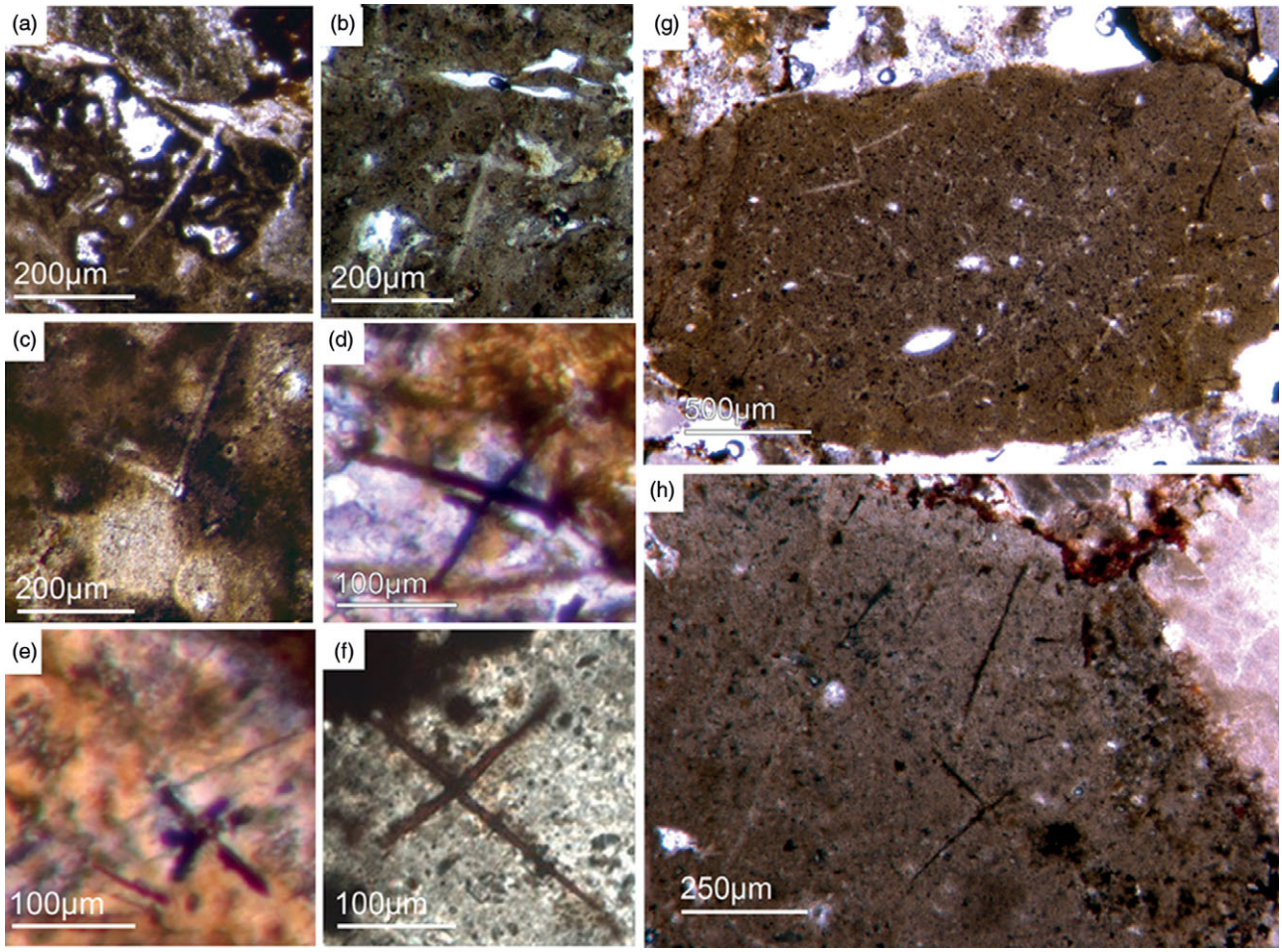

Fig. 2. Hexactinellid spicule types. (a, b) Oblique cuts of regular hexactins (Fon1, 26). (c) Hexatin with preserved axial canals (Fon36). (d) Pentactin and stauractin embedded in yellow-brownish phosphate, preserved in Fe-oxide that derived from pyrite (Fon27). (e) A regular hexactin (Fon29). (f) A stauractin preserved in Fe-oxide embedded in bright phosphatic material (Fon02). (g) Lyssacine hexactinellid skeleton with parenchymal hexactinellid spicules contained in fine-grained dark-brown phosphate (Fon27). (h) Monaxon and pentactin spicules preserved in Fe-oxide (formerly pyrite).

framboidal pyrite. Some spicules are entirely replaced by iron oxide (Fig. 2 d, e, f, h). Silicious spicules tend to be completely recrystallized and are typically overgrown by the first generation of carbonate cement that was then diagenetically phosphatized. In addition to simple hexactins, differentiated triaxon spicules were observed, including (possibly dermal) pentactins (Figs 2d, 3d, 4d), stauractins (Figs 2f, h, 4b) and maybe diactins (Fig. 2h). Differentiation in mega- and microscleres, as seen in the ball-shaped hexactinellids of the Niutitang Formation basal phosphorites in China (Luo & Reitner, 2019), was not observed.

The lyssacine morphotype of nearly articulated hexactinellids displays only weakly developed regularities in spicule arrangement. In some cases, only pentactins and stauractins are located at the sponges' marginal areas ('*Dermalia*' *sensu* Schulze, 1887). The basic hexactins ('*Principalia*' *sensu* Schulze, 1887) are randomly orientated and not attached to each other within the lyssacine sponge tissue (Fig. 3a, b).

This is in contrast to almost entirely preserved hexactinellids that have fused spicule arrangements (Figs 3c, d, 4). The choanosmal spicules in the latter seem to be fused as in cemented skeletons. However, they do not exhibit a rectangular architecture known from typical Dictyospongidae. It is possible to differentiate a few large (0.5 mm) fused hexactins from the abundant smaller ones (250 µm), with the latter being much more abundant (Fig.4a, b). The dermal area exhibits large pentactins (Fig. 4d) and possible tangentially arranged stauractins (Fig. 4b). The sponges are strongly impregnated with light brownish phosphate that likely replaced the primary sponge tissue. The spicules are often surrounded by dark, dense prismatic phosphate, and the inner parts are filled with a bright phosphatic cement (Fig. 4a, b). A second type of preservation displays a brownish phosphatic spicule replacement, though a few have bright phosphatic cements. We observed fused spicule arrangement in a few choanosomal spicules. It is not clear whether this type of preservation is related to rapid phosphatization or if the cementation was mediated by the sponge. If the latter is the case, then this would be the oldest appearance of an advanced rigid hexactinellid skeleton.

5.c. Phylogenetic status of Demospongiae (Sollas, 1885)

Demosponges and hexactinellids are phylogenetically closely related and form a monophylum (e.g. Wörheide *et al.* 2012). The elementary demosponge spicule types are monaxons and a four-rayed spicule called 'caltrops'. The caltrop is an advanced characteristic demosponge spicule (van Kempen, 1990; Reitner & Mehl, 1995, 1996; Reitner & Wörheide, 2002) (Fig. 5a, b, d). Hexactinellids also harbour monaxon spicules. In living sponges,

https://doi.org/10.1017/S001675682100087X Published online by Cambridge University Press

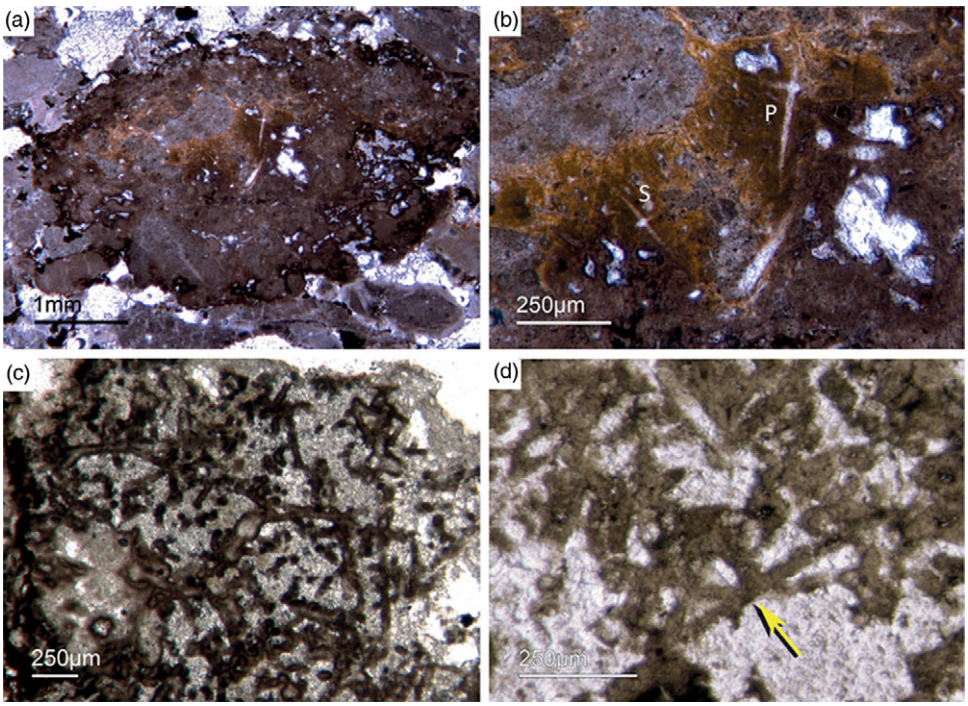

Fig. 3. (a) A lyssacine hexactinellid preserved in honey-yellow phosphate (Fon38). (b) Detail of Figure 6a exhibiting large pentactins (P) and stauractins (S). The honey-yellow phosphate shows in the upper margin a tent-like fabric, indicating that the early rapid phosphatization may have permineralized the soft tissue of the sponge. (c) Cemented parenchymal hexactinellid skeleton (Fon20). (d) Fused hexactinellid skeleton. Primarily articulated fused spicular skeleton, mainly preserved in brownish phosphate (Fon16). Space between spicules cemented by bright phosphate. Remains of dermal skeleton exhibiting fused pentactins (arrow).

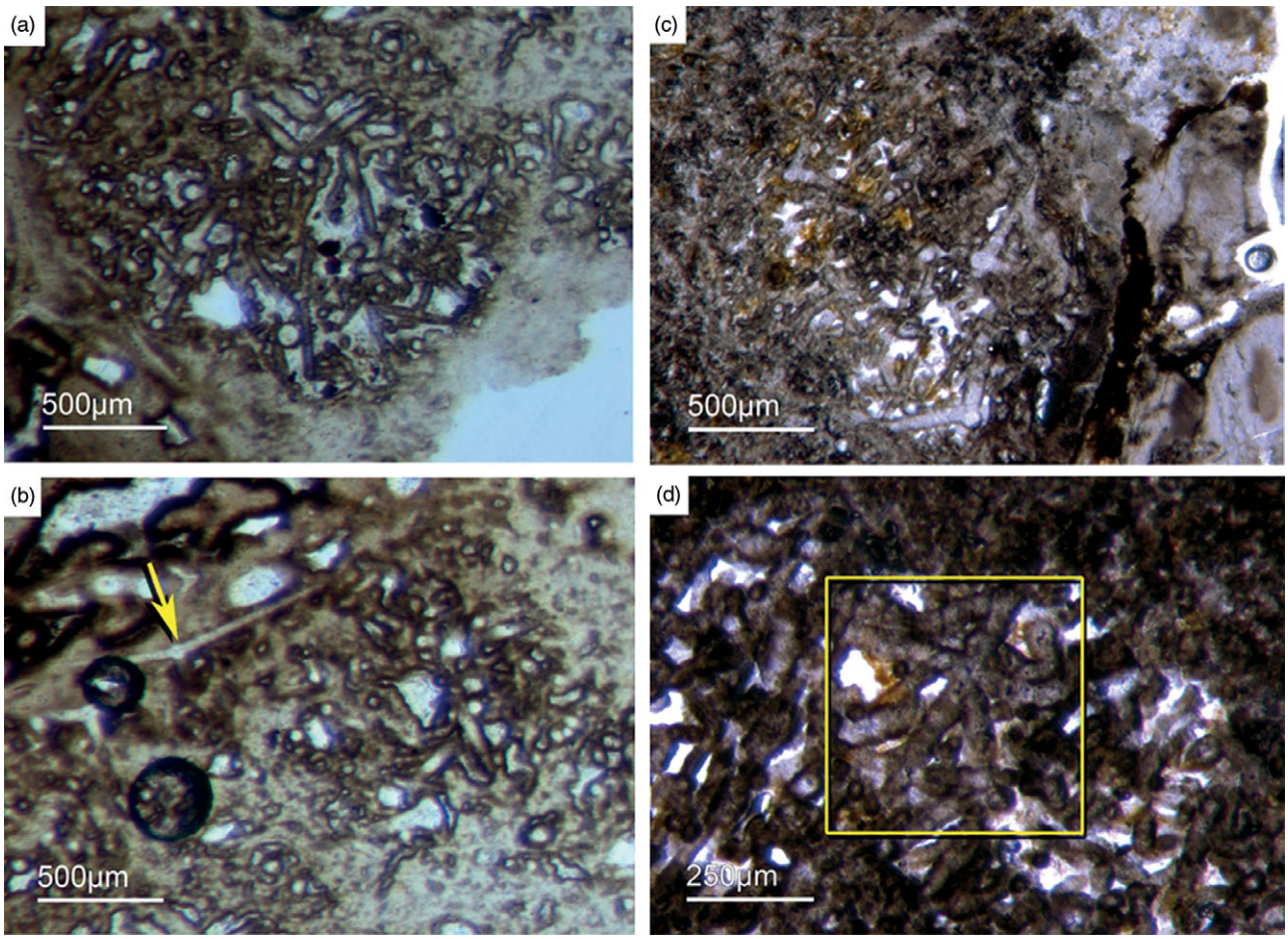

Fig. 4. Fused hexactinellid skeletons. (a, b) Nearly entirely preserved hexactinellid sponge with a cemented parenchymal and dermal spicular skeleton (Fon29). The marginal portions completely impregnated by honey-yellow phosphate and show ghost-remains of spicules and permineralized tissue. Preserved are large dermal spicules like stauractins (arrow in Fig. 7b). (c, d) Best preserved skeleton with large and small parchenchymal hexactin spicules and pentactin dermal spicules (rectangle) (Fig. 7d) (Fon26).

https://doi.org/10.1017/S001675682100087X Published online by Cambridge University Press

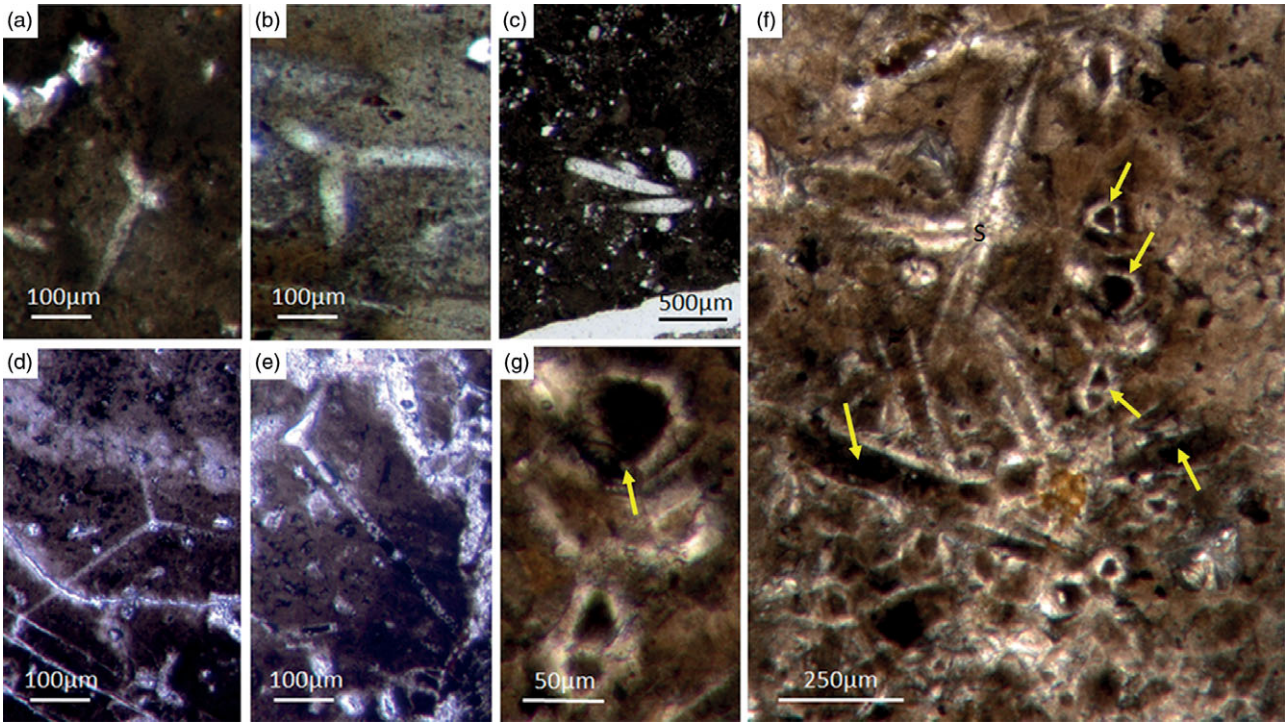

Fig. 5. Basic demosponge spicules. (a, b, d) Various types of four-rayed spicules with an angle of about 120° between the rays (Fon31, 59, 11). (c) Group of thick monaxon-style spicules (Fon11). (e) Typical triaene (orthotriaene) spicule (Fon11). (f, g) Aggregates of spicules (S) with possible remains of enlarged axial filament structure (arrows). Axial canal filled with organic matter (kerogen) and exhibiting hexagonal cross-sections as known from demosponges (Fon10).

it is possible to distinguish between hexactinellid and demosponge monaxons by the cross-section shape of the axial filament: it is more or less quadratic in hexactinellids, while it is triagular or hexagonal in demosponges (e.g. Hartman, 1980; Reitner & Mehl, 1996; Leys *et al.* 2007). In the fossil record, however, this structure is rarely preserved pristinely.

Botting & Muir (2013) illustrated the axial canals of a reticulosan which, in their opinion show hexagonal cross-section. There are several problems with this interpretation. First, the depicted axial canals do not appear to be hexagonal but rather round in shape. Furthermore, the presented data are insufficient to support the conclusion. More specifically, the feature would need to be found in many more fossil sponge taxa to establish a phylogenetic significance. This is an essential prerequisite, since the claimed presence of hexagonal cross-sections in a single taxon could likewise be interpreted as an evolutionary experiment of the specific group. It is thus neither necessarily representative nor a plesiomorphic strait. For these reasons, we do not accept the premature claim that some reticulosans represent stem group demosponges (Botting & Muir 2013, 2018) and refrain from considering it in our discussion. Notably, demosponges are characterized by a great diversity of monaxonic spicule types that are distinctly different to hexactinellid monaxons.

Despite these morphological differences, both sponge clades form spicules by a fairly similar process. More precisely, amorphous hydrated opaline silica is precipitated on an organic matrix that forms a proteinaceous fibre (axial filament). However, the fibre's proteinaceous composition in demosponges is formed of silicatein α, a cathepsin L-like lysosomal proteolytic enzyme (Shimizu *et al.* 1998). In hexactinellids, in contrast, the fibre usually consists of cathepsin instead of silicatein; in only one case a modified silicatein (AuSil-Hex protein in *Aulosaccus schulzei*) was detected (Veremeichik *et al.* 2011). In hexactinellids, collagen is also an important spicule secondary protein (Uriz *et al.* 2003; Müller *et al.* 2007; Ehrlich, 2010). This is in contrast to the sponge clade Calcarea which secrete calcitic spicules extracellularly and not around an organic fibre (Jones, 1970). The capability to form spicules developed multiple times and in phylogenetically independent groups of sponges (Wörheide *et al.* 2012; Voigt *et al.* 2017).

Notably, various demosponges are non-spicular, and such forms were formerly described as 'Keratosa,' or 'horny sponges' (Minchin, 1900; Lévi, 1957). Recent phylogenomic studies have separated the non-spicular taxa into the subclass 'Keratosa' (orders Dendroceratida and Dictyocertida) and the subclass Verongimorpha–Myxospongia (orders Chondrosiida and Verongiida) (Borchiellini *et al.* 2004; Erpenbeck *et al.* 2012; Wörheide *et al.* 2012; Redmond *et al.* 2013; Morrow & Cárdenas, 2015). The organic skeletons of these sponges are mainly composed of spongin, a composite of protein and/or chitin (Ehrlich *et al.* 2017). Spongin is still an enigmatic proteinaceous material that contains halogenated residues and until recently had not been sequenced (Ehrlich, 2019). This composite material is extremly resistant, as demonstrated by findings of chitin in middle Cambrian vauxiid keratose sponges (Ehrlich *et al.* 2013). Luo & Reitner (2014) demonstrated, for the first time, that 'keratose' non-spicular demosponge fossils are abundantly preserved in Phanerozoic carbonates. They showed that the rapid micritization of the soft tissue and relatively slower decay of the spongin–chitin skeleton resulted in spar-filled moulds of the skeleton scaffolds.

5.d. Fontanarejo spicule record of basic Demospongiae

5.d.1. Non-articulated demosponge spicules

Different types of simple isolated four-rayed spicules were found within the Fontanarejo phosphorites (Fig. 5a, b, d). In a few cases, triaene dermal spicules (e.g. orthotrianes), which are likely

https://doi.org/10.1017/S001675682100087X Published online by Cambridge University Press

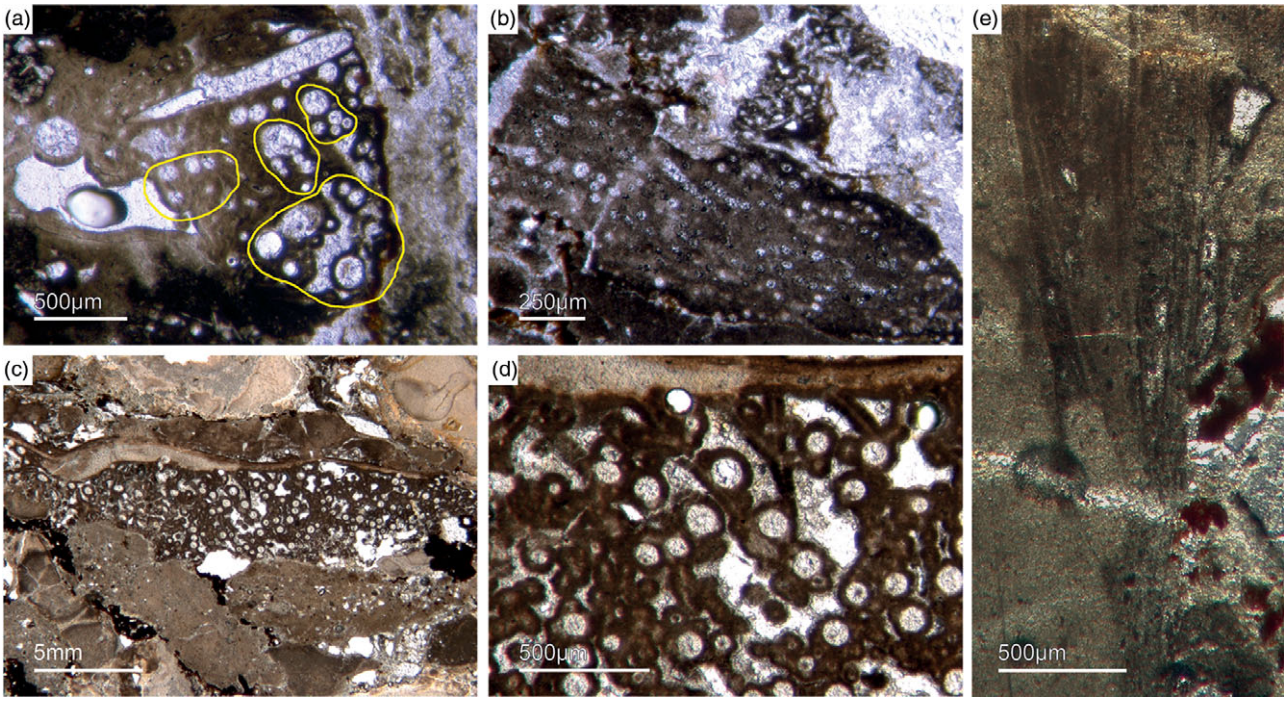

Fig. 6. Articulated demosponge spicular skeletons. (a) Plumose bundle of large styles (Fon1). This arrangement of spicules is known from the 'axinellid–halichondrid' group. (b) Cross-sections of styles that are mostly arranged in rows and probably part of the dermal skeleton (Fon1). In (a, b) the sponges are preserved in honey-yellow to brownish apatite, representing permineralized soft tissue. (c, d) Cross-sections of monaxon spicules grouped in bundles (Fon4). The individual spicules are glued by dark phosphatic cements. The arrangement of upright spicule bundles is known from early Cambrian sponges like *Halichondrites* and *Hamptonia*. (e) A typical hamptonid spicule bundle is formed by very long thin styles (Fon20, 19, 0007).

modified caltrops (Fig. 5e), were recorded. Large, thick spicule styles (*c.* 0.5–1 mm long, 50–100 µm thick) are abundant and often arranged in bundles (Figs 5c, 6a–d). Most of the spicules are embedded in yellow-brownish phosphorite, and often held together by a dark rim of phosphatic cement (Fig. 6a, c, d). Some of the spicules exhibit a clear hexa- to triangular central part formed by organic matter. This part could be the remains of a spicule's central fibre; however, the preservation is unusual (Fig. 5g, f) and not yet understood.

5.d.2. 'Axinellid–halichondrid ' spicule architectures

Some of the observed sponge specimens exhibit well-preserved spicule architecture (Figs 6a, b, c, d, 7c, d). For instance Figure 6a shows an association of thick and small styles with spicule bundles. The plumose arrangement of some of the spicule bundles resembles an ancient 'axinellid' bauplan (e.g. Reitner, 1992; Reitner & Wörheide, 2002). Figure 6b, c and d show cross-cuts through a demosponge dermal layer comprising vertically orientated monaxons. The monaxons are cemented by fibrous brown apatite (Fig.6c, d). In some of the spicules the axial canals are still visible as small dark spots (Fig. 6b, d). Figure 7c and d show a demosponge with plumose bundles of long and short styles in the outer dermal parts and tangentially orientated monaxons in the inner dermal parts (arrow in Fig. 7d). Figures 6e and 7c show further examples of plumose spicule arrangements. The long, thin styles are nearly radially arranged, a structure known from lower Cambrian taxa such as *Choia*, *Choiaella*, *Hamptoniella*, *Hamptonia*, *Halichondrites* and *Pirania* (Reitner & Wörheide, 2002; Finks & Rigby, 2004; Rigby & Collins, 2004; Botting *et al.* 2013). In some cases, bouquet-like arrangements of long styles (some millimetres) are observed close to a plumose arrangement of spicules (Fig. 7d). These bouquet types are present in ball-shaped modern taxa of Tethyidae and closely related to Hemiastrellidae (Hooper, 2002; Sará, 2002; Sorokin *et al.* 2019). A particularly remarkable demosponge specimen exhibits a well-developed, very dense etcosomal spicule architecture composed of short strongyles (*c.* 50 µm) (Fig. 8). The strongyles are interwoven and display a preferred tangential orientation (Fig. 8b, e). The endosomal spicules are large, thick styles (*c.* 200–300 µm long, 50 µm diameter) surrounded by long (200–400 µm), thinner styles (Fig. 8a, c, d). Some accessory curved monaxons are also present. This morphological character is similar to an 'axinellid–halichondrid' sponge type, but the ectosomal dermal layer is unusual.

5.d.3. 'Hadromerid' spicule arrangements

In addition to these spicule arrangements, we observed demosponges with a thick dermal layer of small ball-shaped microscleres (*c.* 10–15 µm), probably former asterose spicule types (Fig. 7a, b). The choanosomal part of these sponges exhibits randomly orientated, poorly preserved monaxone spicules, probably styles (Fig. 7a). This bauplan is known from 'tetractinellid' demosponges. A 'hadromerid' affinity is most probable. In one case, only a dense dermal crust of putative asterose microscleres is observed (Fig. 7e, f). This sponge resembles the modern hadromerid Chondrillidae and the Cretaceous fossil taxon *Calcichondrilla crustans* Reitner 1991, which show similar dermal asterose microsclers (e.g. Reitner, 1991; Boury-Esnault, 2002; Fromont *et al.* 2008).

5.d.4. Putative 'keratose' demosponges

Non-spicular demosponges are a sister group of spicular demosponges (e.g. Maldonado, 2009; Erpenbeck *et al.* 2012;

https://doi.org/10.1017/S001675682100087X Published online by Cambridge University Press

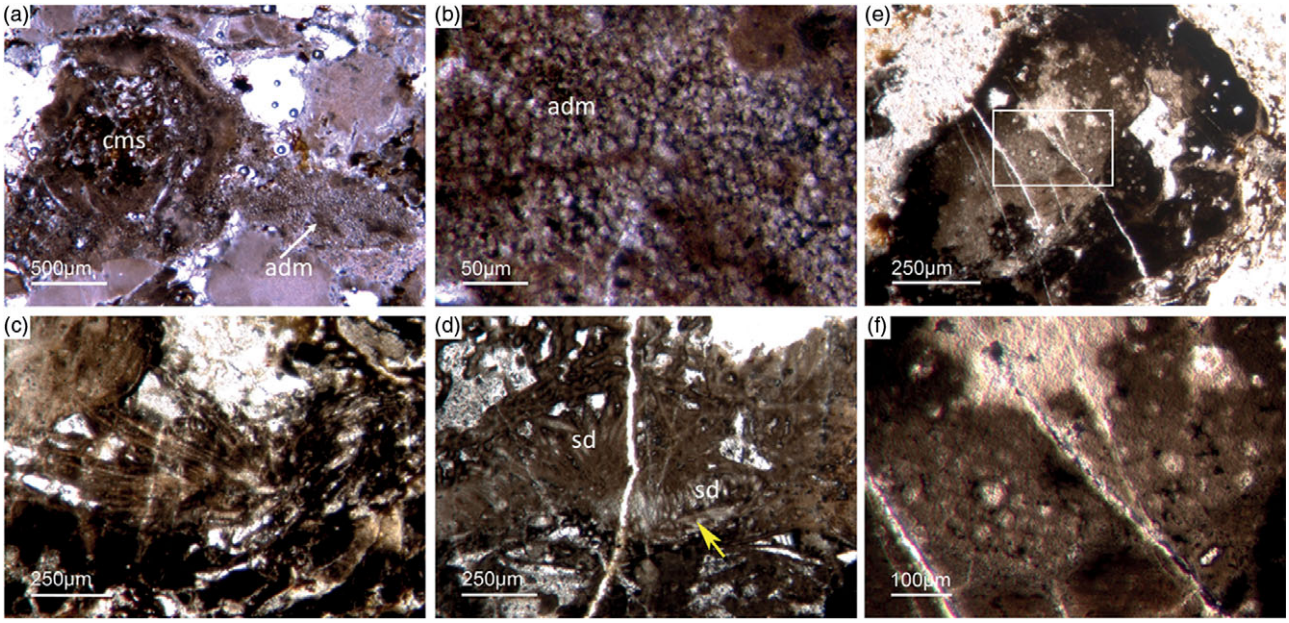

Fig. 7. Articulated demosponge spicular skeletons. (a, b) Representing a 'hadromerid' skeleton. The sponge shows a dense crust of putative asterose dermal microsclers (adm) and randomly orientated choanosomal, probably monaxon spicules (cms) (Fon 38). (c) Radially orientated long styles typical for various early Cambrian sponges like *Choia*, *Choiaella*, *Hamptoniella* (Fon20). (d) Plumose arrangement of short dermal styles (ds) and tangentially arranged monaxons (arrow) on the outer part of the skeleton (Fon20). (e, f) The fossil represents asterose microsclers characteristic for chondrillid hadromerids ((f) enlarged area of (e)) (Fon17).

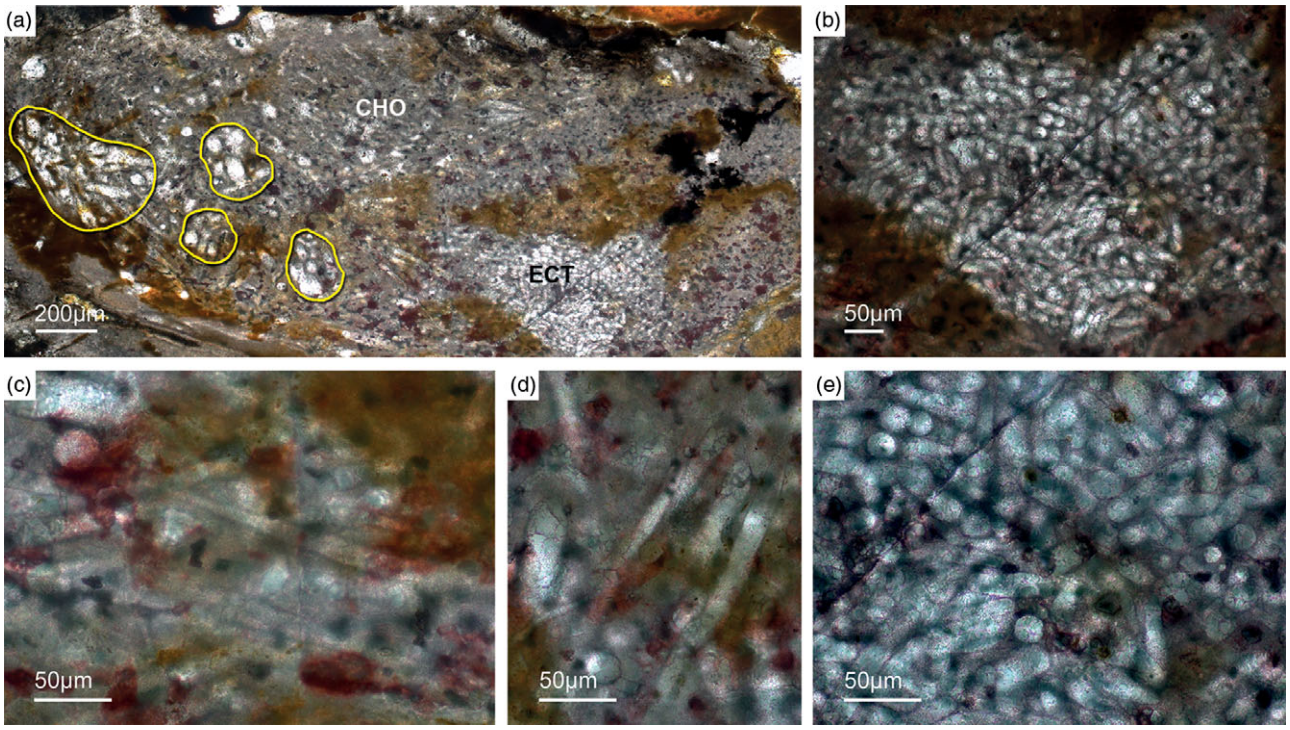

Fig. 8. Almost entirely preserved sponge exhibiting a dense dermal layer (ECT – ectosomal spicules). (a) Plumose arranged thick large styles (yellow lines) within the choanosomal part of the sponge (CHO) and (c, d) smaller styles. (b, e) The dense dermal layer exhibits a network of interwoven short strongyles (ECT) (Fon41).

Morrow & Cárdenas, 2015). Recent investigations demonstrated a widespread fossil record of this group, which is due to the decay-resistant skeletal spongin and chitinous fibres (e.g. Luo & Reitner, 2014, 2016; Friesenbichler *et al.* 2018). The best-known fossil taxon is the middle Cambrian *Vauxia* from the Burgess Shale, which has recently also been discovered in the lower Cambrian Chengjiang Biota (Series 2, Stage 3) (Luo *et al.* 2020). The presence of chitin in this genus is in good accordance with the skeletal composition of the Verongiida (subclass Verongimorpha) (Ehrlich *et al.* 2013).

https://doi.org/10.1017/S001675682100087X Published online by Cambridge University Press

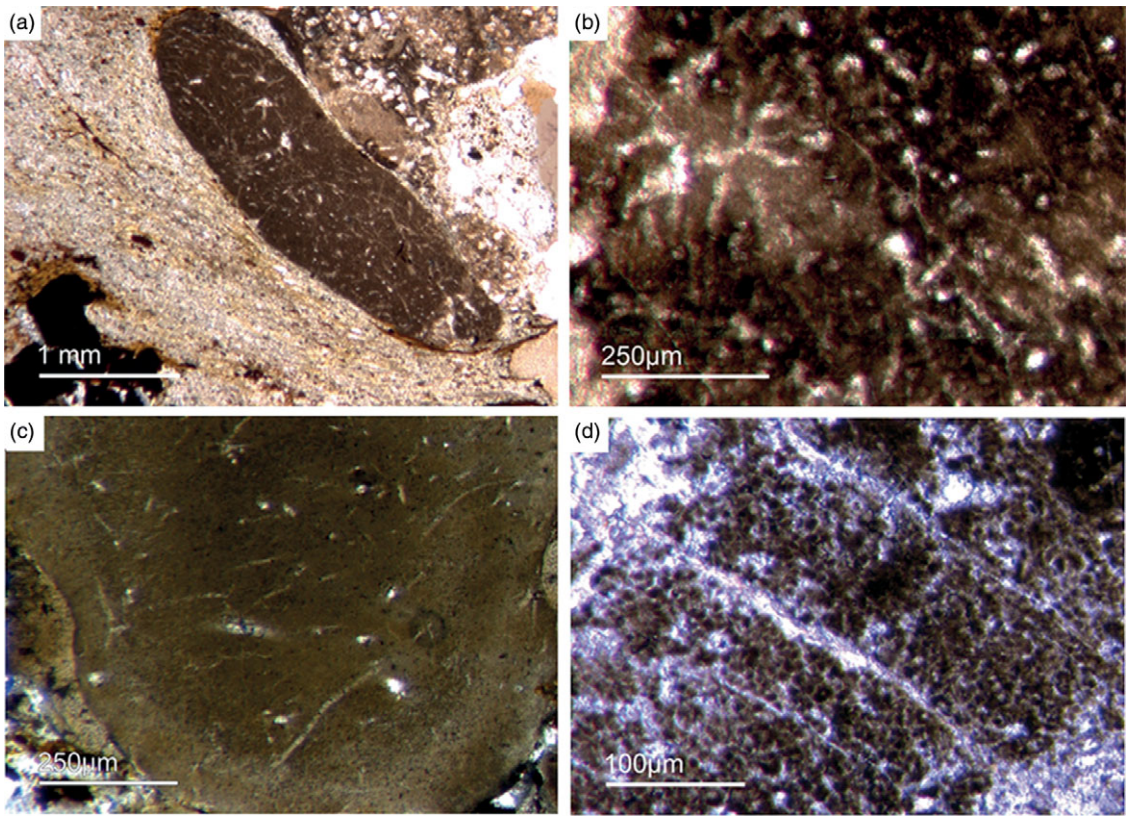

Fig. 9. (a) A dark-brownish phosphorite component with a clear fibre network (Fon19). (b) Network of thin filamentous fabrics within a dark-brownish phosphorite, remarkably similar to typical 'keratose' organic fibre skeletons (Fon77). (c) Within a brownish phosphatic clast thin filamentous fabrics are seen, interpreted as remains of spongin fibres – alternatively, boring traces may also be possible (Fon56). (d) Dark micropeloids enriched in phosphate and organic matter, likely the taphonomic end-product of microbial sponge tissue degradation (Fon16).

Some components in the Fontanarejo phosphorites may be fossils of keratose sponges – (Fig. 9). This is because they exhibit an irregular network of fibres that is remarkably similar to those known from younger Phanerozoic keratose fibre networks (Fig. 9a, b, c). Most of the fibre networks are embedded in dark-brown phosphate matrices. They often form connecting points, and in some cases the fibres are curved. The fibres are preserved as a bright phosphatic cement. Micro-peloids, a characteristic taphonomic end product of sponge tissue alteration (Reitner *et al.* 1995; Reitner & Neuweiler, 1995, Reitner & Schumann-Kindel, 1997), fill the spaces between the fibres (Fig. 9d). All these features are typical characteristics of keratose sponges and are interpreted here accordingly. An alternative interpretation of these structures as boring traces is not favoured here but might be tested in future studies.

5.d.5. Putative sponge larvae or resting bodies

Bundles of long styles with egg-shaped stuctures are observed within a few sponge 'balls' (Fig. 10). These egg-shaped structures have a diameter of *c.* 100–200 µm and resemble viviparous sponge larvae or gemmules. They have a distinct *c.* 10 µm thick bright rim that consists of radially orientated phosphatic crystals, a dark inner granular matrix, and potentially small monaxon spicule remains. The dark inner granular matrix consists of abundant iron oxides (probably remains of pyrite), and dark-grey, irregular phosphatic organic matter. The observed potential spicules are *c.* 20–50 µm long.

A possible (and in our view most suitable) analogue is the parenchymella larva of viviparous demosponges (e.g. known from haplosclerids, poecilosclerids and 'Keratosa'), the only larva type with simple monaxonic spicules (Leys, 2003; Maldonado, 2006; Ereskovsky, 2010). To the best of our knowledge, fossil vivaparous sponge larvae (e.g. parenchymella-type) have not been observed until this study.

Alternatively, the observed structures could be resting bodies like those of gemmulae. Gemmulae structures are very rarerly preserved in the fossil record (Volkmer-Ribeiro & Reitner, 1991; Pronzato *et al.* 2017). Today, marine sponges with gemmulae are also rare and restricted to a few taxa of the Haplosclerida (*Acervochalina loosanoffi*, family Chalinidae) and Hadromerida (*Protosuberites* sp.) (Connes *et al.* 1978; Arp *et al.* 2004).

5.e. Putative small shelly fauna

As already discussed, determining the age of the Fontanarejo phosphorites is a central problem. No stratigraphically important fossils have been previously found within the phosphorite-containing layers, and so the existing age was determined based on sedimentological correlation with nearby geological structures (Pieren Pidal, 2000; Jensen *et al.* 2010; Álvaro *et al.* 2019) and one zircon age published by Talavera *et al.* (2012). Sponge spicules in the phosporites indicate a Cambrian age, but unfortunately do not allow for a more precise biostratigraphic interpretation. From the Alcudia anticline, the early mollusc *Anabarella* was described, providing an important stratigraphic age (Pieren & García-Hidalgo, 1999; Vidal *et al.* 1999; Pieren Pidal, 2000). For the first time, we also found SSF remains in the Fontanarejo phosphorites. Unfortunately, these microfossils could not be isolated due to the

https://doi.org/10.1017/S001675682100087X Published online by Cambridge University Press

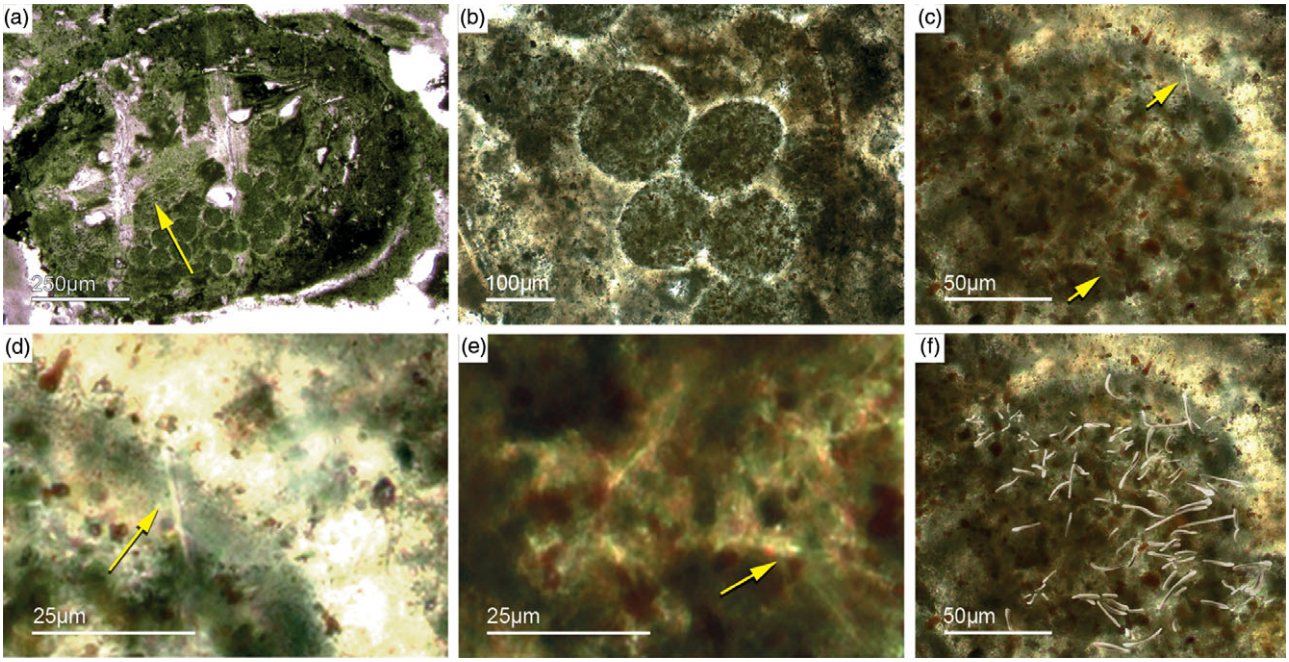

Fig. 10. (a, b) Demosponge with a central bundle of styles associated with abundant egg-shaped structures (Fon 27). (c, e) These egg-shaped bodies show a distinct margin (c) and a central area with abundant small Fe-rich small grains (e). A further important characteristic is abundant small spicules (styles, oxea) (yellow arrows in (c)). (f) Sketch of recognized spicules. The egg-shaped bodies are interpreted as larvae or resting cysts. These bodies show best analogy with demosponge parenchymella larvae.

high amounts of siliceous cement, and therefore have only been examined in thin-sections. However, many specimens observed in the thin-sections show strong similarities to *Anabarella* (Figs 11, 13a), while others classify as tube fossils (Fig. 12a, b). These new micropalaeontological findings match with previous findings from the Alcudia anticline near Ciudad Real (e.g. Pieren Pidal, 2000), and thus provide compelling evidence for a similar stratigraphic age. Furthermore, they are also in agreement with findings of SSFs (including *Anabarella*) that have recently been reported from the Ibor and Alcudia anticlines of the CIZ (Álvaro & Lorenzo, 2021).

One SSF exhibits a chambered structure comparable to phragmocones of cephalopods (Fig. 12c). Up to now the only known SSF with a phragmocone-like structure is the upper Cambrian monoplacophoran *Knightoconus* from Antarctica (Yochelson *et al.* 1973). However, there is a new finding of a cephalopod-type SSF from the early Cambrian (upper Terreneuvian) of Newfoundland (Hildenbrand *et al.* 2021). Together, these fossils indicate an early Cambrian origin of chambered cephalopods. On the other hand, the SFF somewhat resembles the chambered tube of '*Hyolithes kingi*' from the Lower Cambrian of Jordan by Bandel (1986). Another important group of SSFs in the studied materials are tubular remains of mollusc-type organisms. In thin-section we observe simple narrow shafts some millimetres long and 50–100 µm in diameter (Fig. 12a, b). Commonly, we observe cross-sections of putative tubular fossils with a maximum diameter of a few millimetres, often exhibiting a weak outer ornamentation. The shell structure is often prismatic (Fig. 13 b, c).

5.f. Implications of the Fontanarejo record on early metazoan evolution

Molecular clock analyses suggest that sponges evolved in the Neoproterozoic. However, no convincing body fossils or spicules have been reported from that era. For this reason, molecular clocks are usually calibrated with sedimentary hydrocarbons in Cryogenian and Ediacaran rocks and oils that are widely considered as being indicative for sponges (i.e. 24-isopropylcholestanes, 24-icp) (Sperling *et al.* 2010; Erwin *et al.* 2011; Cunningham *et al.* 2016; Gold *et al.* 2016; Dohrmann & Wörheide, 2017). A recently reported steroid biomarker (26-methylstigmastane, 26-mes) might provide additional evidence for early sponges (Zumberge *et al.* 2018). This is because only certain groups of extant demosponges are known to biosynthesize plausible precursor sterols for both of these distinct compounds as major lipids (e.g. Hofheinz & Oesterhelt, 1979; Djerassi & Silva, 1991; Giner, 1993; McCaffrey *et al.* 1994; Love *et al.* 2009; Zumberge *et al.* 2018). However, 24-icp precursors are also known as insignificant (that is, two orders of magnitude less abundant) by-products in the biosynthesis of 24-*n*-propylcholestane lipids by extant pelagophyte algae (Giner *et al.* 2009; Love & Summons, 2015).

Traces of putative 24-ipc and 26-mes precursor in protists (Nettersheim *et al.* 2019) have shortly afterwards been demonstrated to be artefacts formed during closed-system pyrolysis under catalytic conditions (i.e. >300 °C: e.g. Bobrovskiy *et al.* 2021; van Maldegem *et al.* 2021). These high-temperature experiments do not simulate diagenesis accurately and produced traces of 24-ipc and 26-mes along with a complex array of other organic compounds, which is distinctly different to the very selective abundance pattern of C_{30} steranes in the Neoproterozoic–Cambrian rock record. Nevertheless, it might be possible, that low quantities of 24-ipc and 26-mes form diagenetically through secondary alkylation of C_{29} sterols in sedimentary environments (Duda *et al.* 2020). What is important to realize, however, is that all these studies do not provide evidence that modern demosponges are incapable of synthesizing suitable C_{30} steroid precursors. Consequently, they cannot invalidate demosponges as a potential source of C_{30} steranes in Precambrian rocks; at best they might

https://doi.org/10.1017/S001675682100087X Published online by Cambridge University Press

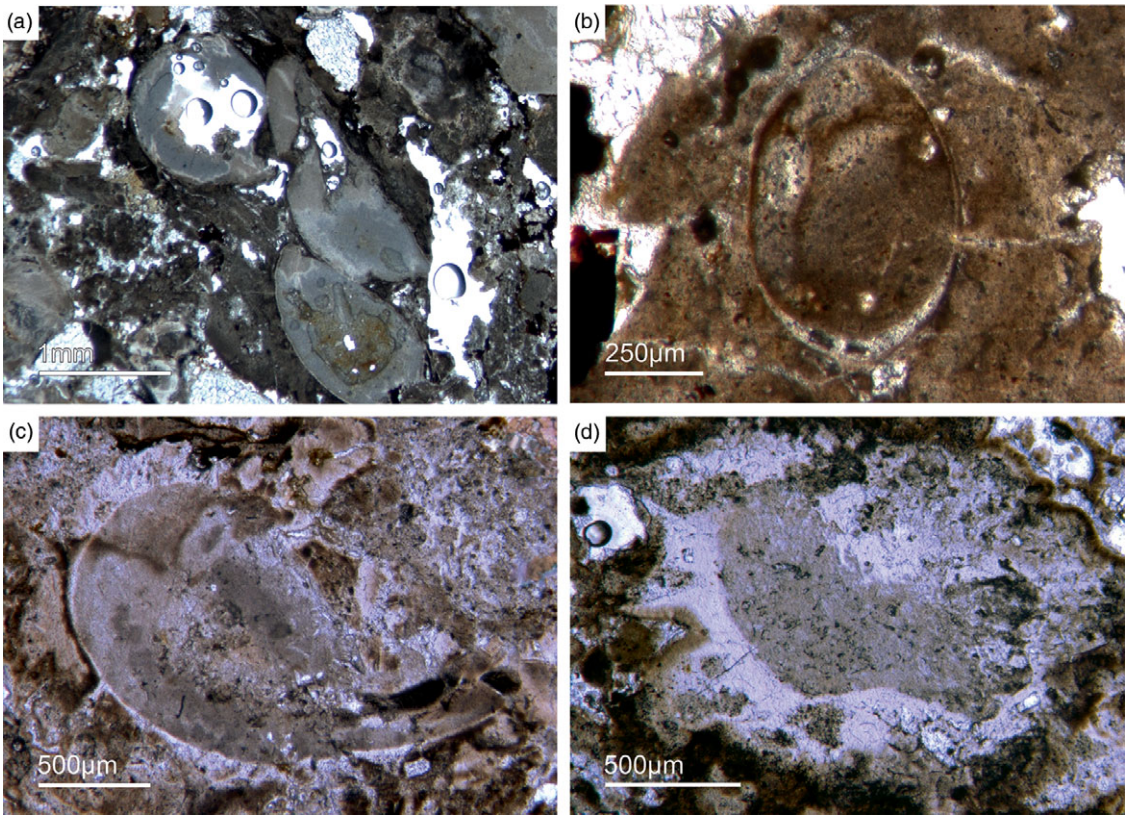

Fig. 11. Mollusc remains. (a, c) Axial and oblique cuts of *Anabarella* sp., a putative monoplacophoran mollusc (Fon61, 35). (b) Vertical cut of *Anabarella* sp. (Fon4), (d) Oblique cut of an ornamented *Anabarella* type (Fon35).

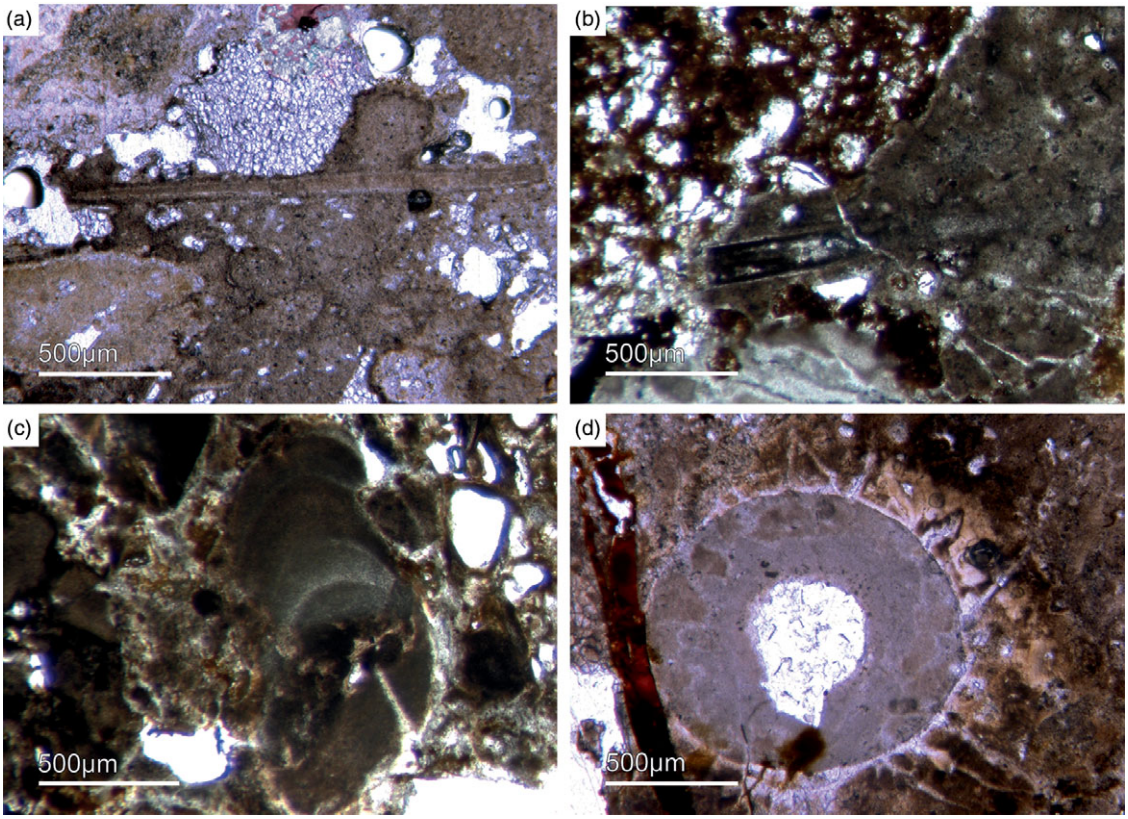

Fig. 12. Multiple types of skeletal fossils. (a, b) Long thin tube shell (Fon99, Fon44, respectively). (c) A new form of a chambered SSF (Fon31). (d) A round cross-section of a tube fossil (Fon78).

https://doi.org/10.1017/S001675682100087X Published online by Cambridge University Press

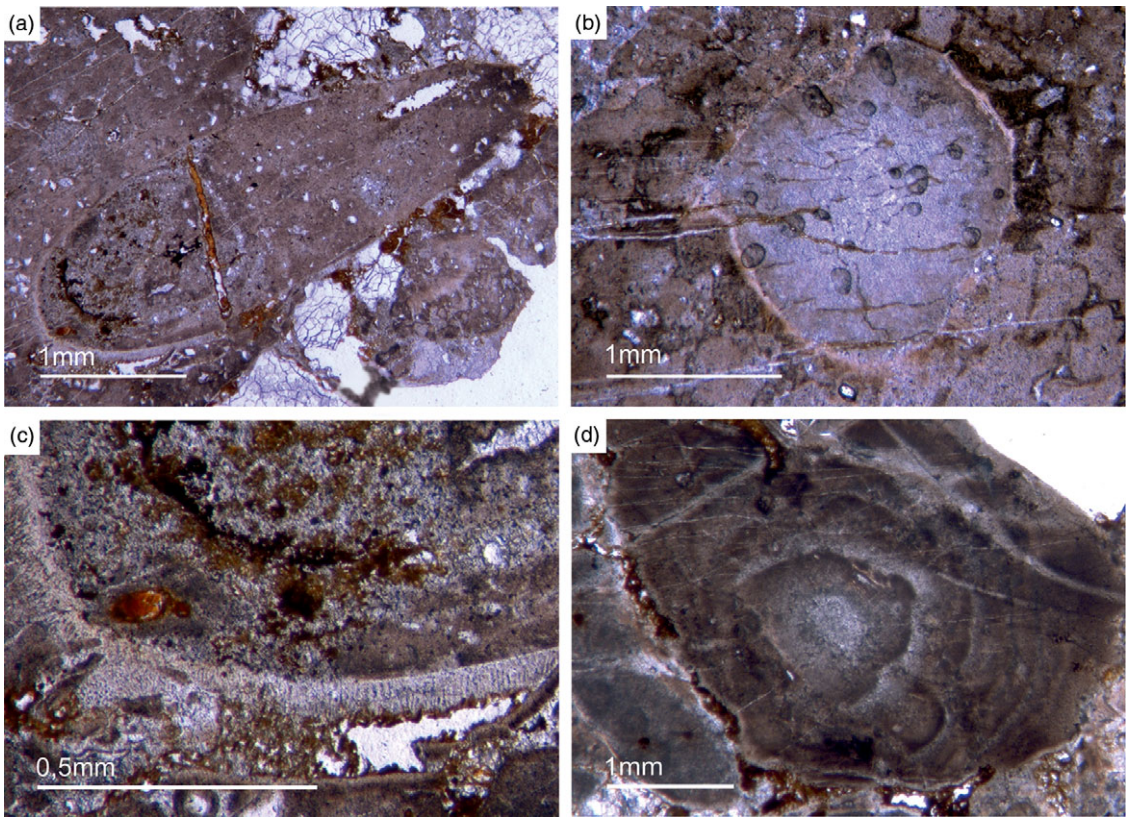

Fig. 13. (a) A median-oblique cut of Anabarella sp. (b) A vertical cut through an ornamented SSF. (c) Detail of the prismatic phosphatic shell structure of Figure 16b (Fon4). (d) Median-oblique cut of a cloudy-colloform microbialite (Fon92).

lower the level of diagnosticity of 24-ipc and 26-mes by establishing additional sources. In summary, the selective abundance pattern of C_{30} steranes is an established characteristic of the late Neoproterozoic–Cambrian rock record, but the interpretation of this feature is controversial and requires further investigation.

Regardless of this debate, our finding of taxonomically diverse demosponge and hexactinellid communities in the late Fortunian Fontanarejo phosphorite further corroborates a Precambrian origin of the phylum Porifera. Notably, the organismic processes involved in biomineralization are enormously complex. Furthermore, there are various extant groups of sponges that seem to belong to the non-spicular lineages and obviously lack a distinct body plan. For all these reasons, it appears likely that the most ancestral representant of the sponge phylum (or 'Urschwamm') solely consisted of soft tissue, perhaps somewhat resembling a microbial mat (Luo & Reitner, 2016). This would be in good agreement with the idea that microbial mats may have transitionally evolved into sponges, as hypothesized earlier (Reitner, 1998). And such a scenario would explain the seeming mismatch between palaeontological findings, the sedimentary hydrocarbon record and molecular clock data.

6. Results and discussion: Sedimentary evidence for microbial-mediated phosphate formation

The abundant cloudy textures observed in the Fontanarejo phosphorite strongly suggest a microbial origin of the deposit, as proposed earlier by Álvaro *et al.* (2016). The microbial impact on sediment formation is further evidenced by a variety of components such as mm-sized aggregates of phosphatic material that exhibit irregular to cauliflower-like shapes and often contain small allochthonous grains as for instance siliciclastic components and spicules. Notably, these components represent up to 20 % of the entire phosphatic sediment. A further example is abundant oncoid-like components with roughly laminated colloform and thrombolitic structures and a distinct nucleus (Figs 13d, 14). Raman spectroscopy revealed the presence of pure and organic-rich apatite, organic matter, as well as of accessory minerals such as anatase (TiO_2), and quartz in these components (Figs S4, S5). The laminated to thrombolitic structures and the close spatial association of organic–inorganic phases indicate that apatite formation was probably mediated via microbial exopolymeric substances (EPS) and/or fuelled by phosphorus deriving from bacterial cell degradation, perhaps in biofilms (see below).

A second type of microbialite is mm-sized micro-domal stromatolites. Generally, the structure of these stromatolites is similar to the colloform structure of the phosphatic oncoid-like components described above. However, the stromatolites exhibit a distinct lamination of alternating, *c.* 50 μm thin dark-brownish, brownish and white layers (Supplementary Fig. S5, in the Supplementary Material available online at https://doi.org/10.1017/S001675682100087X). The dark-brown and brown layers consist of organic-rich and organic-poor apatite, respectively. The white layers, in contrast, are composed of siliceous apatite or pure silica. As in the case of the oncoid-like components (see above), the organic-rich apatite in the stromatolites is likely a product of EPS-controlled mineral precipitation or taphonomic biofilm degradation. Anatase (TiO_2) is enriched in some layers and may have formed authigenically, perhaps even through microbially mediated precipitation; however, unfortunately these processes

https://doi.org/10.1017/S001675682100087X Published online by Cambridge University Press

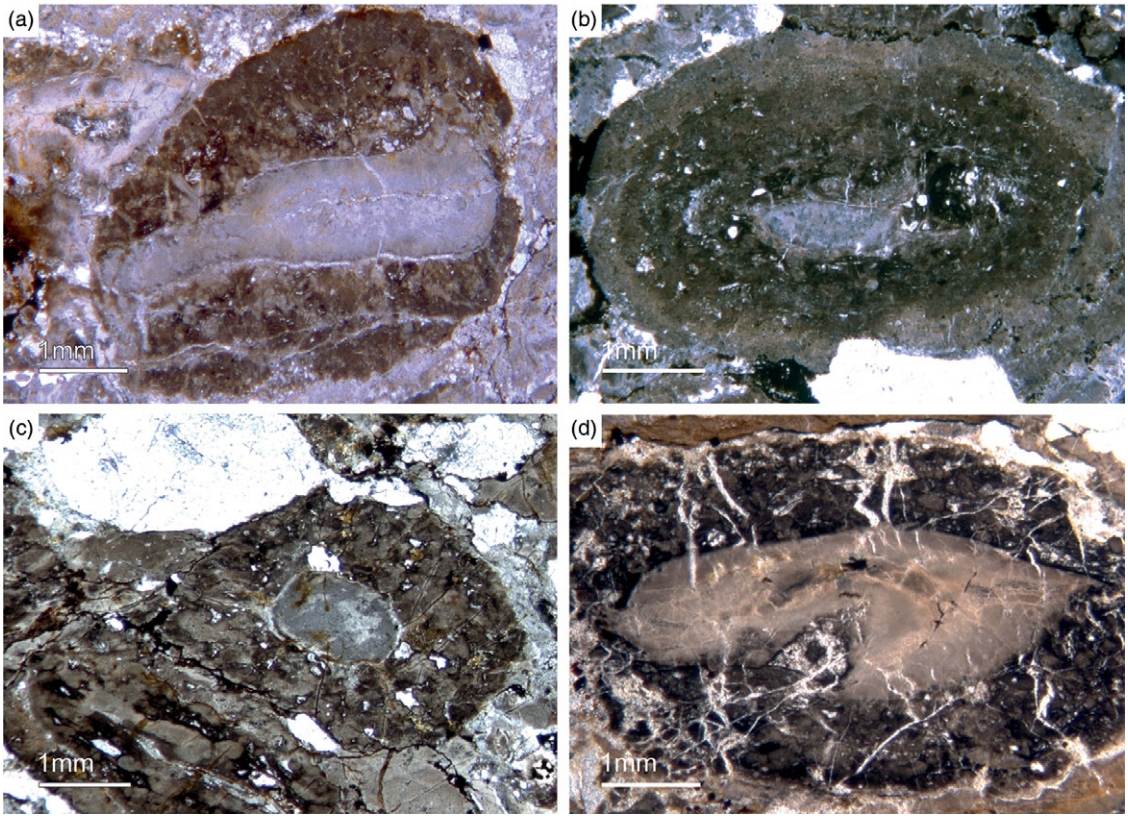

Fig. 14. Oncoid-type microbialites. (a) Encrusting phosphatic microbialite showing an irregular cauliflower growth mode (Fon18). (b) Thrombolitic growth structure on top of phosphatic component (Fon35). (c) Thrombolitic oncoid-type microbialite (Fon44). (d) Dark organic-rich thrombolitic oncoid-type microbialite (Fon21).

are still too poorly understood to draw robust conclusions (e.g. Taran *et al.* 2018; Izawa *et al.* 2019).

The presence of microbes in the Fontanarejo phosphorite environment is further evidenced by large filamentous fossils encapsulated in some of the observed microbialites (Fig. 15a–c). These fossils strongly resemble sheets of extant sulphide-oxidizing bacteria (SOX-B) (Peckmann *et al.* 2004; Bailey *et al.* 2013; Birgel *et al.* 2014; Andreetto *et al.* 2019). This interpretation has important implications for the formation of the Fontanarejo phosphorite deposit. Today, SOX-B are particularly widespread in sediments of coastal upwelling regimes off the west coast of Africa and South America (Arning *et al.* 2009*a*, *b*). Notably, vacuolated SOX-B like the giant bacterium *Thiomargarita* (Schulz & Schulz, 2005) as well as filamentous SOX-B like *Beggiatoa* and *Thioploca* all harbour intracellular polyphosphate inclusions (e.g. Jørgensen & Gallardo, 1999; Brock & Schulz-Vogt, 2011; Salman *et al.* 2011; Crosby & Bailey, 2012). It has been shown that hydrolysis of polyphosphates in *Thiomargarita*-rich sediments releases sufficient phosphor into the pore water to precipitate apatite (Schulz & Schulz, 2005). Moreover, it has been demonstrated by ^{33}P-labelling experiments that phosphate taken up by SOX-B is rapidly transformed from intracellular polyphosphate to apatite (Goldhammer *et al.* 2010). All these studies support the hypothesis that microbial metabolism can foster apatite formation, and we consider this as a plausible explanation for the formation of the Fontanarejo phosphorite.

In non-upwelling systems, apatite formation appears to be linked to a non-microbial process termed 'iron-redox pump' (e.g. Einsele, 1936; Mortimer, 1941; Nürnberg & Peters, 1984; Ruttenberg & Berner, 1993). In anoxic pore-water environments, iron(III) will readily be reduced to iron(II). As a consequence, iron(III)-bearing mineral phases will dissolve, thereby releasing adsorbed phosphor into the pore water, which then further reacts to authigenic apatite. Intriguingly, fresh material from the Pusa shales is locally black and enriched in pyrite, probably indicating low-oxygen conditions (see also Vidal *et al.* 1994). These conditions would have been favourable for an 'iron-redox pump', which thus might account for some of the observed phosphatic cements (Fig. 15d). However, the abundance of evidence for microbial processes still strongly suggests a microbial origin for most of the observed apatite in the Fontanarejo deposit. In combination, both pathways plausibly explain the rapid precipitation of apatite (Cook & Shergold, 1984; Föllmi, 1996) which accounts for the exceptional preservation of microbial features and lyssacine and articulated sponge fossils.

7. Conclusions

1. The Fontanarejo phosphorites were described decades ago, but have not been studied in detail since then. A new detailed geological map is presented in this study, updating and improving previous mappings. The stratigraphic and sedimentological aspects of these deposits have been controversial and are here reviewed and discussed, supporting the interpretation that they are late Fortunian in age and formed as channels of a turbidite system located at the platform–slope transition. Furthermore, we present the first microfacies description of these deposits, and the first comprehensive characterization of their palaeontological content, highlighting the relevance of the contained sponge fossils.

https://doi.org/10.1017/S001675682100087X Published online by Cambridge University Press

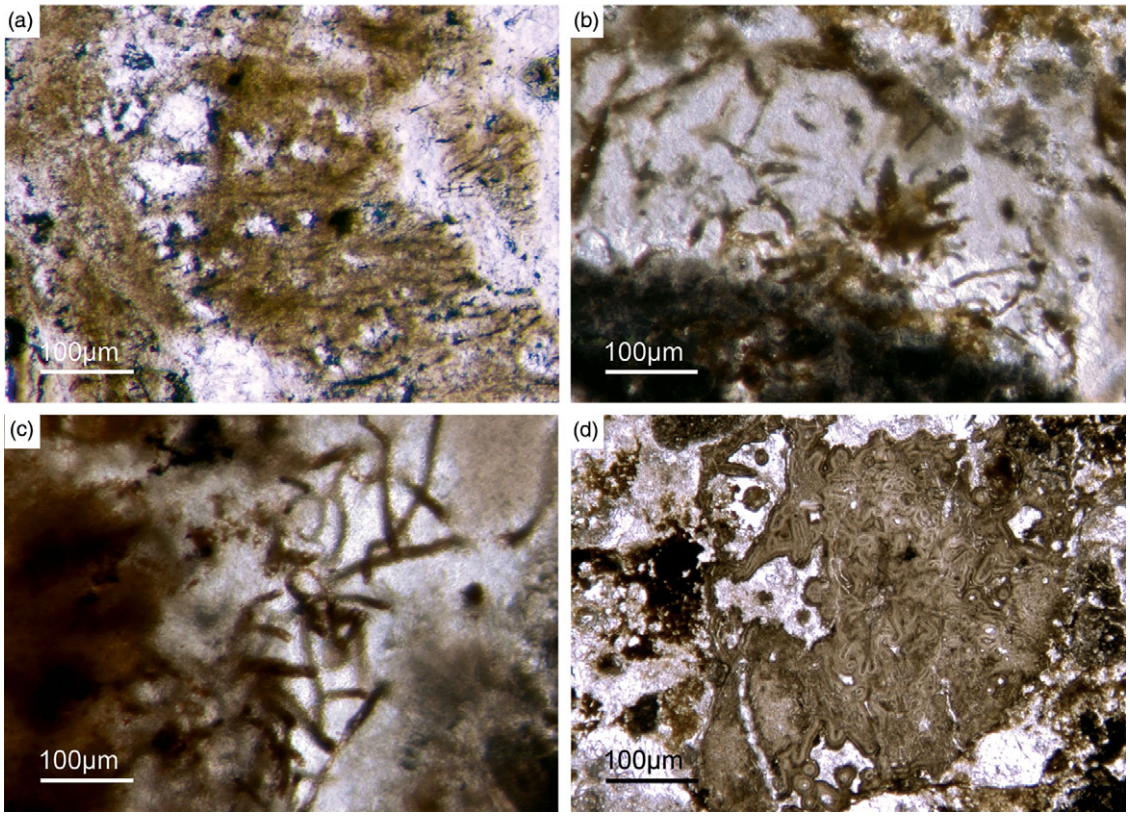

Fig. 15. Filamentous microbial remains. (a) Long filamentous structures, probably remains of sulphide-oxidizing bacteria (SOX-B) (Fon35). (b) Filamentous remains within bright phosphorite (Fon36). (c) Network of large filaments interpreted as remains of SOX-B (Fon36). (d) Sponge skeleton that is strongly cemented by multilayered phosphate, probably resulting from intense flow of P-rich fluids.

2. The phosphorites of Fontanarejo harbour abundant sponge remains. Hexactinellid remains are most abundant, including lyssacine and possible cemented spicular skeletons. In addition to basic hexactins, diactins, stauractins and pentactins are common. The spicules have simple morphologies, and no microsclers were observed. The lyssacine sponges are often preserved in honey-yellow phosphatic material that likely represents permineralized soft tissue. They exhibit only a few parenchymal spicules and, in rare cases, stauractin and pentactin dermal spicules. This type of hexactinellid is related to the 'Rossellimorpha A' *sensu* Mehl-Janussen (1999). In contrast, the hexactinellids with cemented skeletons show bundles of fused hexactins in the parenchymal areas, and also exhibit with hypodermal pentactins.
3. Demosponges are less common but show a higher morphological diversity than hexactinellids. Isolated four-rayed spicules of early demosponges, triaene spicules and diverse monaxonic spicules are common. Articulated plumose and bouquet-type spicule arrangements are related to the 'axinellid–halichondrid' group. An unusual type of an 'axinellid–halichondrid' demosponge was observed that exhibits a dense dermal layer of short strongyles. Two hadromerid-type spicule arrangements were found. One exhibits similarities to chondrillid sponges that possess only large likely dermal asterose-type microsclers. The other displays a well-developed dermal layer of putative asterose microsclers and a choanosomal skeleton of randomly oriented monaxone spicules. Some specimens of putative 'keratose' demosponges were also discovered.
4. The analysed samples contain the SFF *Anabarella* sp. which supports the stratigraphic assignment of the phosphates to the lower Fortunian – Stage 2. In combination, the palaeontological evidence (points 2 and 3 above) and biostratigraphic interpretation of the phosphorites strongly corroborate a Precambrian origin of the phylum Porifera.
5. The phosphatic sediment displays many different fabrics and other structures that are typical characteristics of microbialites. Oncoid-like microbialites are abundant; small domal stromatolites are less common. Both components contain significant amounts of organic matter. Long filamentous structures in some of the samples resemble SOX-B. These features strongly suggest that most of the Fontanarejo apatite was formed via microbial mediation. The inferred rapid precipitation of phosphatic cements was additionally driven by an intense flow of phosphor-rich fluids during early diagenesis. All these processes contributed to the exceptional preservation of fragile sponge skeletons and microbialites.

Acknowledgements. The authors gratefully acknowledge Prof. Dr Sören Jensen, Dr Iván Cortijo (Villuercas-Ibores-Jara UNESCO Global Geopark), Prof. Dr Agustín Pieren, Prof. Dr Marta Rodríguez-Martínez (Univ. Complutense Madrid) and Dr Javier Gonzáles Sanz (IGME, Madrid) for sharing their knowledge with us, and for their continuing support and valuable advice. For technical support we thank Dorothea Hause-Reitner, Axel Hackmann and Yu Pei (University of Göttingen). Ellen Kappel (NY) is thanked for checking the English version of the manuscript. PSG acknowledges the support of a Postdoctoral Fellowship from the Alexander von Humboldt Foundation to stay in Göttingen. JR and J-PD acknowledge the Göttingen Academy of Sciences and Humanities and the University of Göttingen (DFG-Courant Research Center

https://doi.org/10.1017/S001675682100087X Published online by Cambridge University Press

Geobiology) for logistic and financial support. CL thanks the National Natural Science Foundation of China (Grant No. 41972016) for financial support. This is publication no. 11 of the Early Life Research Group (Department of Geobiology, Georg-August-Universität Göttingen; Göttingen Academy of Sciences and Humanities). We thank two reviewers for valuable comments that helped to improve the manuscript.

Declaration of Interest. None.

Supplementary material. To view supplementary material for this article, please visit https://doi.org/10.1017/S001675682100087X

References

Álvaro JJ, Cortijo I, Jensen S, Lorenzo S, Palacios T and Pieren AP (2019) Updated stratigraphic framework and biota of the Ediacaran and Terreneuvian in the Alcudia-Toledo Mountains of the Central Iberian Zone, Spain. *Estudios Geológicos* **75**(2), e093.

Álvaro JJ and Lorenzo S (2021) Cadomian orogenic collapse in the Ibor and Alcudia anticlines of the Central Iberian Zone, Spain. *Geological Magazine*, First View. doi:10.1017/S0016756821000339.

Álvaro JJ, Shields-Zhou GA, Ahlberg P, Jensen S and Palacios T (2016) Ediacaran–Cambrian phosphorites from the western margins of Gondwana and Baltica. *Sedimentology* **63**(2), 350–77.

Andreetto F, Dela Pierre F, Gibert L, Natalicchio M and Ferrando S (2019) Potential fossilized sulfide-oxidizing bacteria in the Upper Miocene sulfur-bearing limestones from the Lorca Basin (SE Spain): paleoenvironmental implications. *Frontiers in Microbiology* **10**. doi:10.3389/fmicb.2019.01031.

Antcliffe JB, Callow RHT and Brasier MD (2014) Giving the early fossil record of sponges a squeeze. *Biological Reviews* **89**(4), 972–1004.

Arning ET, Birgel D, Brunner B and Peckmann J (2009a) Bacterial formation of phosphatic laminites off Peru. *Geobiology* **7**(3), 295–307.

Arning ET, Lückge A, Breuer C, Gussone N, Birgel D and Peckmann J (2009b) Genesis of phosphorite crusts off Peru. *Marine Geology* **262**, 68–81. doi:10.1016/j.margeo.2009.03.006.

Arp G, Reimer A and Reitner J (2004) Microbialite formation in seawater of increased alkalinity, Satonda Crater Lake, Indonesia: reply. *Journal of Sedimentary Research* **74**(2), 318–25.

Bailey JV, Corsetti FA, Greene SE, Crosby CH, Liu P and Orphan VJ (2013) Filamentous sulfur bacteria preserved in modern and ancient phosphatic sediments: implications for the role of oxygen and bacteria in phosphogenesis. *Geobiology* **11**(5), 397–405.

Bandel K (1986) The reconstruction of 'Hyolithes kingi' as annelid worm from the Cambrian of Jordan. *Mitteilungen Geologisch-Paläontologisches Institut Hamburg* **61**, 35–101.

Birgel D, Guido A, Liu, X, Hinrichs K-U, Gier S and Peckmann J (2014) Hypersaline conditions during deposition of the Calcare di Base revealed from archaeal di- and tetraether inventories. *Organic Geochemistry* **77**, 11–21.

Bobrovskiy I, Hope JM, Nettersheim BJ, Volkman JK, Hallmann C. and Brocks JJ (2021) Algal origin of sponge sterane biomarkers negates the oldest evidence for animals in the rock record. *Nature Ecology & Evolution* **5**(2) 165–8.

Borchiellini C, Chombard C, Manuel M, Alivon E, Vacelet J and Boury-Esnault N (2004) Molecular phylogeny of Demospongiae: implications for classification and scenarios of character evolution. *Molecular Phylogenetics and Evolution* **32**(3), 823–37.

Botting JP and Muir LA (2013) Spicule structure and affinities of the Late Ordovician hexactinellid-like sponge Cyathophycus loydelli from the Llanfawr Mudstones Lagerstätte, Wales. *Lethaia* **46**, 454–69.

Botting JP and Muir LA (2018) Early sponge evolution: a review and phylogenetic framework. *Palaeoworld* **27**(1), 1–29.

Botting JP, Muir LA and Lin JP (2013) Relationships of the Cambrian Protomonaxonida (Porifera). *Palaeontologia Electronica* **16**(2), 9A.

Botting JP and Peel JS (2016) Early Cambrian sponges of the Sirius Passet Biota, North Greenland. *Papers in Palaeontology* **2**(4), 463–87.

Boury-Esnault N (2002) Order Chondrisida Boury-Esnault & Lopés, 1985. Family Chondrillidae Gray, 1872. In *Systema Porifera: A Guide to the Classification of Sponges* (eds JNA Hooper and RWM Van Soest), pp. 52–68. New York: Kluwer Academic/Plenum Publishers.

Brain CK, Prave AR, Hoffmann, K-H, Fallic, AE, Botha A, Herd, DA, Sturrock C, Young I, Condon DJ and Allison SG (2012) The first animals: ca. *760-million-year-old sponge-like fossils from Namibia. South African Journal of Science* **108**(1/2), 658–65.

Brasier MD, Green O and Shields G (1997) Ediacarian sponge spicule clusters from southwestern Mongolia and the origins of the Cambrian fauna. *Geology* **25**(4), 303–6.

Brasier MD, Perejón A and De San José (1979) Discovery of an important fossiliferous Precambrian-Cambrian sequence in Spain. *Estudios Geológicos* **35**, 379–83.

Brock J and Schulz-Vogt H N (2011) Sulfide induces phosphate release from polyphosphate in cultures of a marine Beggiatoa strain. *The ISME Journal* **5**, 497–506.

Chang S, Feng Q, Clausen S and Zhang L (2017) Sponge spicules from the lower Cambrian in the Yanjiahe Formation, South China: the earliest biomineralizing sponge record. *Palaeogeography, Palaeoclimatology, Palaeoecology* **474**, 36–44.

Chang S, Zhang L, Clausen S, Bottjer DJ and Feng Q (2019) The Ediacaran-Cambrian rise of siliceous sponges and development of modern oceanic ecosystems. *Palaeogeography, Palaeoclimatology, Palaeoecology* **333**, 105438.

Chen J, Hou X and Li G (1990) New lower Cambrian demosponges – Quadrolaminiella gen. nov. from Chengjiang, Yunnan. *Acta Palaeontologica Sinica* **29**(4), 402–14.

Chen J, Hou X and Lu H (1989) Lower Cambrian leptomitids (Demospongea), Chengjiang, Yunnan. *Acta Palaeontologica Sinica* **28**(1), 17–30.

Clites EC, Droser ML and Gehling JG (2012) The advent of hard-part structural support among the Ediacara biota: Ediacaran harbinger of a Cambrian mode of body construction. *Geology* **40**(4), 307–10.

Connes R, Carriére D and Paris J (1978) Étude du développement des gemmules chez la demosponge marine Suberites domuncula (Olivi) Nardo. *Annales des Sciences Naturelles, Zoologie, Paris* **20**(4), 357–87.

Cook PJ and Shergold JH (1984) Phosphorus, phosphorites and skeletal evolution at the Precambrian–Cambrian boundary. *Nature* **308**, 231–36.

Crosby CH and Bailey JV (2012) The role of microbes in the formation of modern and ancient phosphatic mineral deposits. *Frontiers in Microbiology* **3**, 241. doi:10.3389/fmicb.2012.00241.

Cunningham JA, Liu AG, Bengtson S and Donoghue PCJ (2016) The origin of animals: can molecular clocks and the fossil record be reconciled? *BioEssays* **39**, 1–12.

Díez Balda MA, Vegas R and Gonzáles Lodeiro F (1990) Structure, autochthonous sequences of Central Iberian Zone. In *Pre-Mesozoic Geology of Iberia* (eds RD Dallmeyer and E Martínez García), pp. 172–88. Berlin: Springer-Verlag.

Ding W-M and Qian Y (1988) Late Sinian to early Cambrian small shelly fossils from Yangjiaping, Shimen, Hunan. *Acta Micropalaeontologica Sinica* **5**(1), 39–55.

Djerassi C and Silva CJ (1991) Biosynthetic studies of marine lipids. *Accounts of Chemical Research* **24**(12), 371–8.

Dohrmann M, Janussen D, Reitner J, Collins AG and Wörheide G (2008) Phylogeny and evolution of glass sponges (Porifera, Hexactinellida). *Systematic Biology* **57**(3), 388–405.

Dohrmann M, Kelley C, Kelly M, Pisera A, Hooper JNA and Reiswig HM (2017) An integrative systematic framework helps to reconstruct skeletal evolution of glass sponges (Porifera, Hexactinellida). *Frontiers in Zoology* **14**(1), 18. doi:10.1186/s12983-017-0191-3.

Dohrmann M and Wörheide G (2017) Dating early animal evolution using phylogenomic data. *Scientific Reports* **7**(1). 3599.

Duda J-P, Love GD, Rogov VI, Melnik DS, Blumenberg M and Grazhdankin DV (2020) Understanding the geobiology of the terminal Ediacaran Khatyspyt Lagerstätte (Arctic Siberia, Russia). *Geobiology* **18**(6), 643–62.

Ehrlich H (2010) Chitin and collagen as universal and alternative templates in biomineralization. *International Geology Review* **52**(7–8), 661–99.

Ehrlich H (2019) Enigmatic structural protein spongin. In *Marine Biological Materials of Invertebrate Origin* (ed. H Ehrlich), pp. 161–72. Biologically-Inspired Systems 13. Berlin and Heidelberg: Springer.

Ehrlich H, Bazhenov VV, Debitus C, de Voogd N, Galli R, Tsurkan MV, Wysokowski M, Meissner H, Bulut E, Kaya M and Jesionowski T (2017) Isolation and identification of chitin from heavy mineralized skeleton of Suberea clavata (Verongida: Demospongiae: Porifera) marine demosponge. *International Journal of Biological Macromolecules* **104**, 1706–12.

Ehrlich H, Rigby JK, Botting JP, Tsurkan MV, Werner C, Schwille P, Petrášek Z, Pisera A, Simon P, Sivkov VN, Vyalikh DV, Molodtsov SL, Kurek D, Kammer M, Hunoldt S, Born R, Stawski D, Steinhof A, Bazhenov V and Geisler T (2013) Discovery of 505-million-year old chitin in the basal demosponge Vauxia gracilenta. *Scientific Reports* **3**, 3497.

Einsele W (1936) Über die Beziehungen des Eisenkreislaufs zum Phosphatkreislauf im eutrophen See. *Archiv für Hydrobiologie* **29**, 664–86.

Ereskovsky AV (2010) *The Comparative Embryology of Sponges*. Dordrecht: Springer Netherlands, 323 pp.

Erpenbeck D, Galitz A, Ekins M, Cook S de C, van Soest RWM, Hooper JNA and Wörheide G (2020) Soft sponges with tricky tree: on the phylogeny of dictyoceratid sponges. *Journal of Zoological Systematics and Evolutionary Research* **58**(1), 27–40.

Erpenbeck D, Sutcliffe P, Cook S de C, Dietzel A, Maldonado M, van Soest RWM, Hooper JNA and Wörheide G (2012) Horny sponges and their affairs: on the phylogenetic relationships of keratose sponges. *Molecular Phylogenetics and Evolution* **63**(3), 809–16.

Erpenbeck D and Wörheide G (2007) On the molecular phylogeny of sponges (Porifera). *Zootaxa* **1668**, 107–26.

Erwin DH, Laflamme M, Tweedt SM, Sperling EA, Pisani D and Peterson KJ (2011) The Cambrian Conundrum: early divergence and later ecological success in the early history of animals. *Science* **334**, 1091–7.

Finks RM and Rigby JK (2004) Paleozoic demosponges. In *Treatise on Invertebrate Paleontology, Part E Porifera, vol. 3* (eds RM Finks, REH Reid and JK Rigby), pp. 9–173, Boulder, Colorado, and Lawrence, Kansas: Geological Society of America and University of Kansas.

Föllmi KB (1996) The phosphorus cycle, phosphogenesis and marine phosphate-rich deposits. *Earth-Science Reviews* **40**(1–2), 55–124.

Friesenbichler E, Richoz S, Baud A, Krystyn L, Sahakyan L, Vardanyan S, Peckmann J, Reitner J and Heindel K (2018) Sponge-microbial buildups from the lowermost Triassic Chanakhchi section in southern Armenia: microfacies and stable carbon isotopes. *Palaeogeography, Palaeoclimatology, Palaeoecology* **490**, 653–72.

Fromont J, Usher KL, Sutton DC, Toze S and Kuo J (2008) Species of the sponge genus Chondrilla (Demospongiae: Chondrosida: Chondrillidae) in Australia. *Records of the Western Australian Museum* **24**(4), 469–86.

Gabaldón López V, Hernández Urroz, J, Lorenzo Álvarez S, Picard Boira J, Santamaría Casanova J and Solé Pont FJ (1989) Sedimentary facies and stratigraphy of Precambrian-Cambrian phosphorites on the Valdelacasa anticline, Central Iberian Zone, Spain. In *Phosphate Deposits of the World, vol. 2: Phosphate Rock Resources* (eds AJG Notholt, RP Sheldon and DF Davidson), pp. 422–8. Cambridge: Cambridge University Press.

Gehling JG and Rigby JK (1996) Long-expected sponges from the Neoproterozoic Ediacara Fauna, Pound Subgroup, South Australia. *Journal of Paleontology* **70**, 185–95.

Giner JL (1993) Biosynthesis of marine sterol side chains. *Chemical Reviews* **93**(5), 1735–52.

Giner JL, Zhao H, Boyer GL, Satchwell MF and Andersen RA (2009) Sterol chemotaxonomy of marine pelagophyte algae. *Chemistry & Biodiversity* **6**, 1111–30.

Gold DA, Grabenstatter J, Mendoza A de, Riesgo A, Ruiz-Trillo I and Summons R (2016) Sterol and genomic analyses validate the sponge biomarker hypothesis. *Proceedings of the National Academy of Sciences* **113**(10), 2684–9.

Goldhammer T, Brüchert V, Ferdelman TG and Zabel M (2010) Microbial sequestration of phosphorus in anoxic upwelling sediments. *Nature Geoscience* **3**(8), 557–61.

Guo J, Li Y, Han J, Zhang X, Zhang Z, Ou Q, Liu J, Shu D, Maruyama S and Komiya T (2008) Fossil association from the Lower Cambrian Yanjiahe Formation in the Yangtze Gorges area, Hubei, South China. *Acta Geologica Sinica* **82**(6), 1124–32.

Gutiérrez-Marco JC, Lorenzo S and Sá AA (2017) Fontanarejo (Ciudad Real): una localidad icnológica excepcional del Ordovícico Inferior en los Montes de Toledo meridionales. *Geogaceta* **62**, 47–50.

Hartman WD (1980) Systematics of the porifera. In *Living and Fossil Sponges, Notes for a Short Course* (eds WD Hartman, JW Wendt and F Wiedenmayer), pp. 24–51. Sedimenta 8. Miami: Rosenstiel School of Marine and Atmospheric Science.

Hildenbrand A, Austermann G, Fuchs D, Bengston P and Stinnesbeck W (2021) A potential cephalopod from the early Cambrian of Eastern Newfoundland, Canada. *Communications Biology* **4**, 388.

Hofheinz W and Oesterhelt G (1979) 24-isopropylcholesterol and 22-Dehydro-24-isopropylcholesterol, novel sterols from a sponge. *Helvetica Chimica Acta* **62**(4), 1307–9.

Hooper JNA (2002) Family Hemiasterellidae Lendenfeld, 1889. In *Systema Porifera: A Guide to the Classification of Sponges* (eds JNA Hooper and RWM Van Soest), pp. 186–95. New York: Kluwer Academic/Plenum Publishers.

Hooper JNA and Van Soest RWM (2002) *Systema Porifera: A Guide to the Classification of Sponges*. New York: Kluwer Academic / Plenum Publishers. 1707 pp.

Izawa MRM, Banerjee NR, Shervais JW, Flemming RL, Hetherington CJ, Muehlenbachs K, Schultz C, Das D and Hanan BB (2019) Titanite mineralization of microbial bioalteration textures in Jurassic volcanic glass, Coast Range Ophiolite, California. *Frontiers in Earth Science* **7**, 315. doi:10.3389/feart.2019.00315.

Jensen S, Palacios T and Mus MM (2010) Revised biochronology of the Lower Cambrian of the Central Iberian zone, southern Iberian massif, Spain. *Geological Magazine* **147**(5), 690–703.

Jones WC (1970) The composition, development, form and orientation of calcareous sponge spicules. In *The Biology of the Porifera* (ed. WG Fry), pp. 91–123. Symposium of the Zoological Society 25. London: Academic Press.

Jørgensen BB and Gallardo VA (1999) Thioploca spp.: filamentous sulfur bacteria with nitrate vacuoles. *FEMS Microbiology Ecology* **28**(4), 301–13.

Lee WL, Reiswig HM, Austin WC and Lundsten L (2012) An extraordinary new carnivorous sponge, Chondrocladia lyra, in the new subgenus Symmetrocladia (Demospongiae, Cladorhizidae), from off of northern California, USA. *Invertebrate Biology* **131**(4), 259–84.

Lévi C (1957) Ontogeny and systematics in sponges. *Systematic Zoology* **6**, 174–83.

Leys SP (2003) Comparative study of spiculogenesis in demosponge and hexactinellid larvae. *Microscopy Research and Technique* **62**(4), 300–11.

Leys SP, Mackie GO and Reiswig HM (2007) The biology of glass sponges. *Advances in Marine Biology* **52**, 1–147.

Li C-W, Chen J-Y and Hua T-E (1998) Precambrian sponges with cellular structures. *Science* **279**, 879–82.

Liñán E, Gozalo R, Palacios T, Gámez Vinaned JA, Ugidos JM and Mayoral E (2002) Cambrian. In *The Geology of Spain* (eds W Gibbons and T Moreno), pp. 17–29. London: The Geological Society.

López Díaz F (1994) Estratigrafía de los materiales anteordovícicos del anticlinal de Navalpino (Zona Centroibérica). *Revista de la Sociedad Geológica de España* **7**, 31–45.

López Díaz F (1995) Late Precambrian series and structures in the Navalpino Variscan Anticline (Central Iberian Peninsula). *Geologische Rundschau* **84**, 151–63.

Love GD and Summons RE (2015) The molecular record of Cryogenian sponges – a response to Antcliffe (2013). *Palaeontology* **58**, 1131–6.

Love GD, Grosjean E, Stalvies C, Fike DA, Grotzinger JP, Bradley AS, Kelly AE, Bhatia M, Meredith W, Snape CE, Bowring SA, Condon DJ and Summons RE (2009) Fossil steroids record the appearance of Demospongiae during the Cryogenian period. *Nature* **457**, 718–21.

Luo C, Pan B and Reitner J (2017) Chambered structures from the Ediacaran Dengying Formation, Yunnan, China: comparison with the Cryogenian analogues and their microbial interpretation. *Geological Magazine* **154**(6), 1269–84.

Luo C and Reitner J (2014) First report of fossil 'keratose' demosponges in Phanerozoic carbonates: preservation and 3-D reconstruction. *Naturwissenschaften* **101**(6), 467–77.

Luo C and Reitner J (2016) 'Stromatolites' built by sponges and microbes – a new type of Phanerozoic bioconstruction. *Lethaia* **49**(4), 555–70.

Luo C and Reitner J (2019) Three-dimensionally preserved stem-group hexactinellid sponge fossils from lower Cambrian (Stage 2) phosphorites of China. *PalZ* **93**, 187–94.

Luo C, Zhao F and Zeng H (2020) The first report of a vauxiid sponge from the Cambrian Chengjiang Biota. *Journal of Paleontology* **94**(1), 28–33.

Maldonado M (2006) The ecology of the sponge larva. *Canadian Journal of Zoology* **84**(2), 175–94.

Maldonado M (2009) Embryonic development of verongid demosponges supports the independent acquisition of spongin skeletons as an alternative to the siliceous skeleton of sponges. *Biological Journal of the Linnean Society* **97**, 427–47.

Maloof AC, Rose CV, Beach R, Samuelsson BM, Calmet CC, Erwin DH, Poirier GR, Yao N and Simons FJ (2010) Possible animal-body fossils in pre-Marinoan limestones from South Australia. *Nature Geoscience* **3**, 653–9.

Martínez Catalán JR, Martínez Poyatos D and Bea F (2004) Zona Centroibérica. In *Geología de España* (ed. JA Vera), 68–133. Madrid: Instituto Geológico y Minero de España.

McCaffrey MA, Moldowan MJ, Lipton PA, Summons RE, Peters KE, Jeganathan A and Watt DS (1994) Paleoenvironmental implications of novel C30 steranes in Precambrian to Cenozoic Age petroleum and bitumen. *Geochimica et Cosmochimica Acta* **58**(1), 529–32.

Mehl D (1996) Phylogenie und Evolutionsökologie der Hexactinellida (Porifera) im Paläozoikum. *Geologische Paläontologische Mitteilungen der Universität Innsbruck* **4**, 1–55.

Mehl-Janussen D (1999) Die frühe Evolution der Porifera: Phylogenie und Evolutionsökologie der Poriferen im Paläozoikum mit Schwerpunkt der desmentragenden Demospongiae ('Lithistide'). *Münchner Geowissenschaftliche Abhandlungen (A)* **37**, 1–72.

Minchin EA (1900) Sponges. In *A Treatise on Zoology. Part II. The Porifera and Coelenterata* (ed. ER Lankester), pp. 1–178. London: Adam & Charles Black.

Monteserín López V, Nozal Martín F, López Díaz J, Rubio Pascual FJ and Serrano García A (1989) *Mapa Geológico de España, escala 1:50.000. Hoja 735, El Robledo*. Madrid: IGME.

Morrow C and Cárdenas P (2015) Proposal for a revised classification of the Demospongiae (Porifera). *Frontiers in Zoology* **12**, 7. doi:10.1186/s12983-015-0099-8.

Mortimer CH (1941) The exchange of dissolved substances between mud and water in lakes. *Journal of Ecology* **29**, 280–329.

Müller WEG, Li J, Schröder HC, Qiao L and Wang X (2007) The unique skeleton of siliceous sponges (Porifera; Hexactinellida and Demospongiae) that evolved first from the Urmetazoa during the Proterozoic: a review. *Biogeosciences* **4**, 219–32.

Muscente AD, Hawkins AD and Xiao S (2015) Fossil preservation through phosphatization and silicification in the Ediacaran Doushantuo Formation (South China): a comparative synthesis. *Palaeogeography, Palaeoclimatology, Palaeoecology* **434**, 46–62.

Nettersheim BJ, Brocks JJ, Schwelm A, Hope JM, Not F, Lomas M, Schmidt C, Schiebel R, Nowack ECM, De Deckker P, Pawlowski J, Bowser SS, Bobrovskiy I, Zonneveld K, Kucera M, Stuhr M and Hallmann C (2019) Putative sponge biomarkers in unicellular Rhizaria question an early rise of animals. *Nature Ecology & Evolution* **3**(4), 577–81.

Nürnberg GK and Peters RH (1984) Biological availability of soluble reactive phosphorus in anoxic and oxic freshwater. *Canadian Journal of Fisheries and Aquatic Sciences* **41**, 757–65.

Peckmann J, Thiel V, Reitner J, Taviani M, Aharon P and Michaelis W (2004) A microbial mat of a large sulfur bacterium preserved in a Miocene methane-seep limestone. *Geomicrobiology Journal* **21**(4), 247–55.

Peng SC, Babcock LE and Ahlberg L (2020) The Cambrian Period. In *Geologic Time Scale 2020, vol. 2* (eds FM Gradstein, JG Ogg, MD Schmitz and GM Ogg), pp. 565–629. Amsterdam: Elsevier.

Perconig E, Vázquez Guzmán F, Velando F and Leyva F (1983) Sobre el descubrimiento de fosfatos sedimentarios en el Precámbrico Superior de España. *Boletín Geológico y Minero* **94**, 187–207.

Perconig E, Vázquez Guzmán F, Velando F and Leyva F (1986) Proterozoic and Cambrian phosphorites deposits: Fontanarejo, Spain. In *Phosphate Deposits of the World, vol. 1: Proterozoic and Cambrian Phosphorites* (eds PJ Cook and JH Shergold), pp. 220–34. Cambridge: Cambridge University Press.

Picart Boira J (1988) Facies e interpretación de los yacimientos fosfatados del Cámbrico inferior de Fontanarejo, Zona Centro-Ibérica (Ciudad Real). *2 Congreso Español de Geología, Comunicaciones* **1**, 157–60.

Pieren AP and García-Hidalgo JF (1999) El Alcudiense Superior del anticlinal de Alcudia revisitado (Ciudad Real, España central). In *Annual Meeting of IGCP Project 376 (Laurentia–Gondwana connections before Pangea) Extended Abstracts*, 207–214. Cambridge: Cambridge Publications.

Pieren Pidal AP (2000) *Las sucesiones anteordovícias de la region orientel de la provincial de Badajoz y área contigua de la de Ciduad Real*. Doctoral thesis, Universidad Computense de Madrid, Madrid, Spain. https://eprints.ucm.es/id/eprint/5512

Pronzato R, Pisera A and Manconi R (2017) Fossil freshwater sponges: taxonomy, geographic distribution, and critical review. *Acta Palaeontologica Polonica* **62**(3), 467–95.

Redmond NE, Morrow CC, Thacker RW, Diaz MC, Boury-Esnault N, Cárdenas P, Hajdu E, Lôbo-Hajdu G, Picton BE, Pomponi SA, Kayal E and Collins AG (2013) Phylogeny and systematics of Demospongiae in light of new Small-subunit ribosomal DNA (18S) sequences. *Integrative and Comparative Biology* **53**(3), 388–415.

Reid REH (1958) *A Monograph of the Upper Cretaceous Hexactinellida of Great Britain and Northern Ireland, part I*. London: Palaeontographical Society, 46 pp.

Reitner J (1991) Phylogenetic aspects and new descriptions of spicule-bearing hadromerid sponges with a secondary calcareous skeleton (Tetractinomorpha, Demospongiae). In *Fossil and Recent Sponges* (eds J Reitner and H Keupp), pp. 179–211, Berlin and Heidelberg: Springer.

Reitner J (1992) 'Coralline Spongien': Der Versuch einer phylogenetisch-taxonomischen Analyse. *Berliner Geowissenschaftliche Abhandlungen (Reihe E)* **1**, 1–352.

Reitner J (1998) Early Proterozoic microbial benthic community: Basic Sponge Model. *Jahrbuch der Akademie der Wissenschaften zu Göttingen* **1998**, 230–5.

Reitner J and Luo C (2019) Phosphorites as a new window to early Cambrian evolution of sponges: Fontanarejo, central Sapin and basal Niutitang Formation, Hunan, China. *IMECT Short Abstracts, Estudios Geológicos* **75**(2), p002, 34–6.

Reitner J, Luo C and Duda JP (2012) Early sponge remains from the Neoproterozoic-Cambrian phosphate deposits of the Fontanarejo area (central Spain). *Journal of Guizhou University (Natural Sciences)* **29**(Supp. 1), 184–6.

Reitner J and Mehl D (1995) Early Paleozoic diversification of sponges: new data and evidences. *Geologisch-paläontologische Mitteilungen Innsbruck* **20**, 335–47.

Reitner J and Mehl D (1996) Monophyly of the Porifera. *Verhandlungen des Naturwissenschaftlichen Vereins in Hamburg* **36**, 5–32.

Reitner J and Neuweiler F (1995) Mud mounds: a polygenetic spectrum of fine-grained carbonate buildups. *Facies* **32**, 1–70.

Reitner J, Neuweiler F and Gautret P (1995) Modern and fossil automicrites: implications for mud mound genesis. In *Mud Mounds: A Polygenetic Spectrum of Fine-Grained Carbonate Buildups* (eds J Reitner and F Neuweiler), Facies 32, 4–17. Heidelberg, Berlin: Springer.

Reitner J and Schumann-Kindel G (1997) Pyrite in mineralized sponge tissue – product of sulfate reducing sponge-related bacteria? *Facies* **36**, 272–6.

Reitner J and Wörheide G (2002) Non-lithistid fossil Demospongiae: origins of their palaeobiodiversity and highlights in history of preservation. In *Systema Porifera: A Guide to the Classification of Sponges* (eds JNA Hooper and RWM Van Soest), pp. 52–68. New York: Kluwer Academic / Plenum Publishers.

Rigby JK (1986) *Sponges of the Burgess Shale (Middle Cambrian), British Columbia*. Palaeontographica Canadiana monograph (no. 2), 105 pp.

Rigby JK and Collins D (2004) *Sponges of the Middle Cambrian Burgess Shale and Stephen Formations, British Columbia*. Toronto: Royal Ontario Museum Contributions in Science 1, 155 pp.

Rigby JK and Hou X-G (1995) Lower Cambrian demosponges and hexactinellid sponges from Yunnan, China. *Journal of Paleontology* **69**(6), 1009–19.

Rodríguez Alonso MD, Díez Balda MA, Perejón A, Pieren A, Liñan E, López Díaz F, Moreno F, Gámez Vintaned JA, González Lodeiro F, Martínez

Poyatos D and Vegas R (2004) La secuencia litoestratigráfica del Neoproterozoico-Cámbrico Inferior, Dominio del Complejo Esquisto-Grauváquico. In *Geología de España* (ed. A Vera), pp. 78–81, Madrid: Sociedad Geológica de España – Instituto Geológico y Minero de España.

Ruttenberg KC and Berner RA (1993) Authigenic apatite formation and burial in sediments from non-upwelling, continental margin environments. *Geochimica et Cosmochimica Acta* **57**(5), 991–1007.

Salman V, Amann R, Girnth A.-C, Polerecky L, Bailey J, Høgslund S, Jessen G, Pantoja S and Schulz-Vogt HN (2011) A single-cell sequencing approach to the classification of large, vacuolated sulfur bacteria. *Systematic and Applied Microbiology* **34**(4), 243–59.

San José MA (1984) Los materiales anteordovícicos de Anticlinal de Navalpino (provincias de Badajoz y Ciudad Real, España central). *Cuadernos de Geología Ibérica* **9**, 81–117.

San José MA, Pieren AP, García-Hidalgo JF, Vilas L, Herranz P, Peláez J and Perejón A (1990) Ante-Ordovician Stratigraphy, autochthonous sequences of Central Iberian Zone. In *Pre-Mesozoic Geology of Iberia* (eds DR Dallmeyer and E Martínez García), pp. 147–59, Berlin: Springer-Verlag.

Sará A (2002) Familiy Tethyidae Gray, 1848. In *Systema Porifera: A Guide to the Classification of Sponges* (eds JNA Hooper and RWM Van Soest), pp. 245–65. New York: Kluwer Academic / Plenum Publishers.

Schmidt O (1870) *Grundzüge einer Spongien-Fauna des atlantischen Gebietes*. Leipzig: Wilhelm Engelmann, 88 pp.

Schulz HN and Schulz HD (2005) Large sulfur bacteria and the formation of phosphorite. *Science* **307**, 416–18.

Schulze FE (1886) Über den Bau und das System der Hexactinelliden. *Abhandlungen der Königlichen Akademie der Wissenschaften zu Berlin (Physikalisch-Mathematisch Classe)* **1886**, 1–97.

Schulze FE (1887) Report on the Hexactinellida collected by H.M.S. Challenger during the years 1873–76. In Thomson CW. and Murray J, *Report of the Scientific Results of the Voyage of H.M.S. Challenger during the Years 1873–76 under the Command of Captain George S. Nares and Captain Frank Tourle Thomson*, pp. 1–513. Zoology 21. London, Edinburgh and Dublin: Her Majesty's Government.

Serezhnikova EA and Ivantsov YA (2007) Fedomia mikhaili: a new spicule-bearing organism of sponge grade from the Vendian (Ediacaran) of the White Sea, Russia. *Palaeoworld* **16**(4), 319–24.

Shimizu K, Cha J, Stucky GD and Morse DE (1998) Silicatein α: Cathepsin L-like protein in sponge biosilica. *Proceedings of the National Academy of Sciences* **95**(11), 6234–8.

Sollas WJ (1885) A classification of the sponges. *Annals and Magazine of Natural History, Series 5*, **16**(95), 1–395. doi:10.1080/00222938509459901.

Sorokin SJ, Ekins MG, Yang Q and Cárdenas P (2019) A new deep-water Tethya (Porifera, Tethyida, Tethyidae) from the Great Australian Bight and an updated Tethyida phylogeny. *European Journal of Taxonomy* **529**, 1–26.

Sperling EA, Robinson JM, Pisani D and Peterson KJ (2010) Where's the glass? Biomarkers, molecular clocks, and microRNAs suggest a 200-Myr missing Precambrian fossil record of siliceous sponge spicules. *Geobiology* **8**(1), 24–36.

Steiner M, Mehl D, Reitner J and Erdtmann B-D (1993) Oldest entirely preserved sponges and other fossils from the Lowermost Cambrian and a new facies reconstruction of the Yangtze platform (China). *Berliner Geowissenschaftliche Abhandlungen E* **9**, 293–329.

Tabachnick KR (1991) Adaption of the hexactinellid sponges to deep-sea life. In *Fossil and Recent Sponges* (eds J Reitner and H Keupp), pp. 378–86, Berlin and Heidelberg: Springer-Verlag.

Tabachnick KR and Menshenina LL (2002) Family Hyalonematidae Gray, 1857. In *Systema Porifera: A Guide to the Classification of Sponges* (eds JNA Hooper and RWM Van Soest), pp. 1232–63. New York: Kluwer Academic / Plenum Publishers.

Talavera C, Montero P, Martínez Poyatos D and Williams IS (2012) Ediacaran to Lower Ordovician age for rocks ascribed to the Schist–Graywacke Complex (Iberian Massif, Spain): evidence from detrital zircon SHRIMP U–Pb geochronology. *Gondwana Research* **22**(3), 928–42.

Taran M, Rad M and Alavi M (2018) Biosynthesis of TiO_2 and ZnO nanoparticles by Halomonas elongata IBRC-M 10214 in different conditions of medium. *BioImpacts* **8**(2), 81–9.

Uriz M-J, Turon X, Becerro MA and Agell G (2003) Siliceous spicules and skeleton frameworks in sponges: origin, diversity, ultrastructural patterns, and biological functions. *Microscopy Research and Technique* **62**(4), 279–99.

Valladares MI, Barba P and Ugidos JM (2002) Precambrian. In *Geology of Spain* (eds W Gibbons and T Moreno), pp. 7–16. London: The Geological Society of London.

van Kempen TMG (1990) The oldest tetraxon megasclers. In *New Perspectives in Sponge Biology* (ed. K Rützler), pp. 9–16, Washington, DC: Smithsonian Institution Press.

van Maldegem LM, Nettersheim BJ, Leider A, Brocks JJ, Adam P, Schaeffer P, and Hallmann C (2021). Geological alteration of Precambrian steroids mimics early animal signatures. *Nature Ecology & Evolution* **5**(2), 169–73.

Veremeichik GN, Shkryl YN, Bulgakov VP, Shedko SV, Kozhemyako VB, Kovalchuk SN, Krasokhin VB, Zhuravlev YN and Kulchin YN (2011) Occurrence of a silicatein gene in glass sponges (Hexactinellida: Porifera). *Marine Biotechnology* **13**(4), 810–19.

Vidal G, Palacios T, Gámez-Vintaned JA, Balda MAD and Grant SWF (1994) Neoproterozoic–early Cambrian geology and palaeontology of Iberia. *Geological Magazine* **131**(6), 729–65.

Vidal G, Palacios T, Moczydłowska M and Gubanov AP (1999) Age constraints from small shelly fossils on the early Cambrian terminal Cadomian Phase in Iberia. *GFF* **121**(2), 137–43.

Voigt O, Adamska M, Adamski M, Kittelmann A, Wencker L and Wörheide G (2017) Spicule formation in calcareous sponges: coordinated expression of biomineralization genes and spicule-type specific genes. *Scientific Reports 7*, 45658.

Volkmer-Ribeiro C and Reitner J (1991) Renewed study of the type material of Palaeospongilla chubutensis Ott and Volkheimer (1972). In *Fossil and Recent Sponges* (eds J Reitner and H Keupp), pp. 121–33. Berlin and Heidelberg: Springer-Verlag.

Wallace MW, Hood AvS, Woon EMS, Hoffmann K-H and Reed CP (2014) Enigmatic chambered structures in Cryogenian reefs: the oldest sponge-grade organisms? *Precambrian Research* **255**, 109–23.

Wörheide G, Dohrmann M, Erpenbeck D, Larroux C, Maldonado M, Voigt O, Borchiellini C and Lavrov DV (2012) Deep phylogeny and evolution of sponges (phylum Porifera). In *Advances in Marine Biology* (eds MA Becerro, MJ Uriz, M Maldonado and T Xavier), pp. 1–78, London: Academic Press.

Xiao SH, Hu H, Yuan XL, Parsley RL and Cao R (2005) Articulated sponges from the Lower Cambrian Hetang Formation in southern Anhui, South China: their age and implications for the early evolution of sponges. *Palaeogeography, Palaeoclimatology, Palaeoecology* **220**(1–2), 89–117.

Yin Z, Zhu M, Davidson EH, Bottjer DJ, Zhao F and Tafforeau P (2015) Sponge grade body fossil with cellular resolution dating 60 Myr before the Cambrian. *Proceedings of the National Academy of Sciences* **112**(12), E1453–60.

Yochelson EL, Flower RH and Webers GF (1973) The bearing of the new Late Cambrian monoplacophoran genus Knightoconus upon the origin of the Cephalopoda. *Lethaia* **6**(3), 275–309.

Zumberge JA, Love GD, Cárdenas P, Sperling EA, Gunasekera S, Rohrssen, M, Grosjean E, Grotzinger JP and Summons RE (2018) Demosponge steroid biomarker 26-methylstigmastane provides evidence for Neoproterozoic animals. *Nature Ecology & Evolution* **2**(11), 1709–14.